Received 30 April 2023; revised 24 May 2023; accepted 5 June 2023. Date of publication 30 June 2023; date of current version 5 July 2023.

Digital Object Identifier 10.1109/OJCOMS.2023.3285541

Secondary User Access Control (SUAC) via Quadratic Programming in Massive MIMO Cognitive Radio Networks

HUAXIA WANG [1] (Member, IEEE), AND YU-DONG YAO [2] (Fellow, IEEE)

[1]College of Engineering, Architecture, and Technology, Oklahoma State University, Stillwater, OK 74074, USA

[2]Department of Electrical and Computer Engineering, Stevens Institute of Technology, Hoboken, NJ 07030, USA

CORRESPONDING AUTHOR: H. WANG (e-mail: wanghuaxia2008@gmail.com)

ABSTRACT In cognitive radio (CR) networks, a secondary user access control (SUAC) technique has been designed to enhance spectrum efficiency, in which a jamming signal is deliberately injected to maintain reliable sensing performance of authorized secondary users (A-SUs) and degrades unauthorized secondary users (UA-SUs) spectrum sensing results. We consider the problem of jamming signal design in massive multiple-input multiple-output (MIMO) CR networks wherein each primary user has a larger number of antennas that coexists with multiple secondary users. In this paper, we propose a jamming signal design framework that combines maximizing the jammer's influences on UA-SUs and minimizing on A-SUs. The resulting problem is a non-convex quadratically constrained quadratic programming (QCQP) problem, and a semidefinite relaxation (SDR) method can be one of the approximate solutions but cannot meet our stringent constraints and lacks jamming efficiency. We propose a novel optimization algorithm based on the K-best methodology to design the jamming signal. Simulation results show the effectiveness of the proposed K-best based SUAC method in improving the spectrum sensing performance of A-SUs.

INDEX TERMS Cognitive radio (CR), massive MIMO, spectrum sensing, access control, quadratic programming.

I. INTRODUCTION

IN TRADITIONAL wireless communications systems, there exist significant spectrum under-utilization problems, where some spectrum bands are heavily occupied while others are kept vacant for a long time. Cognitive radio (CR) technology has been introduced to address this issue [1]. Specifically, there are two types of users in the CR network: primary user (PU) and secondary user (SU). Secondary users are allowed to access the spectrum only when the PUs are not utilizing that spectrum. Therefore, one of the crucial tasks in CR is spectrum sensing in order to enhance the spectrum efficiency [2], [3].

The cognitive radio network is very vulnerable to malicious user attacks due to its open and dynamic nature [4], [5], [6]. For example, [4] proposes a primary user emulation attack model, where attackers imitate the PU's behavior and mislead other SUs' spectrum access decisions. In [6], a most active band (MAB) attack model is presented where an attacker selects and performs a denial-of-service (DoS) attack on a spectrum band with the most activities. Thus, it is important to design a robust CR system that maintains PUs/SUs communications quality under severe malicious user attacks. In [7], a secondary user access control (SUAC) framework has been introduced. Two types of secondary users are investigated in SUAC: authorized secondary users (A-SUs) and unauthorized secondary users (UA-SUs). When PU is inactive and vacant in the spectrum, only A-SUs are authorized to utilize the spectrum. To assure a reliable spectrum sensing performance for A-SUs and atrocious sensing results for UA-SUs, a carefully designed jamming signal is injected at the transmission end, where such jamming pattern can only be obtained by A-SUs to eliminate the jamming signal influence when performing spectrum sensing task. To consider A-SUs with different spectrum access priority levels, [8] proposes

a prioritized SUAC (P-SUAC) mechanism. Reference [9] presents the secondary user access control technique in a massive multiple-input multiple-output (MIMO) communications environment, where a jamming signal is generated from a PU transmitter based on the estimated channel state information (CSI) which has a small or negligible influence on A-SUs. The proposed jamming signal design optimization technique is within the quadratically constrained quadratic programs (QCQP) domain with a semi-definite relaxation (SDR) solution provided in [10], [11].

Sparse representation provides a powerful emerging model for signals, where a data source is approximated with a linear combination of a few atoms from an over-complete dictionary [12]. The theory of compressive sensing (CS) has shown that a sparse signal can be reconstructed exactly from many few measurements [13]. Since then, intensive research on sparse signal and data processing have been investigated in the area of wireless communications [14], such as compressive channel estimation in massive MIMO [15], compressive spectrum sensing in CR networks [16], and compressive sensing enabled large-scale wireless sensor networks (WSNs) [17]. Massive data and connectivity are expected to be supported in the next-generation wireless communications systems, such a huge amount of data transmission and storage brings tremendous challenges in signal processing in massive MIMO communications systems.

Motivated by the proposed research in SUAC and the sparse representation research for wireless communications, the objective of this paper is to explore sparse jamming signal design for SUAC in cognitive radio networks by exploiting quadratic programming. The proposed jamming signal design is a sparse representation technique, where the majority of the jamming signal weights are zero. This implies that the proposed sparse jamming signal design approach is greener. In this paper, we consider the secondary user access control model in a massive MIMO communications environment and propose a jamming signal design approach that utilizes uplink CSI between the PU and SUs. To design the jamming signal, an optimization problem is considered and we show that such a non-convex optimization problem can be optimally solved in some special cases. In addition to that, we show that an alternative solution to solve our non-convex problem can be determined through a K-best method based technique [18]. Specifically, K is a tunable parameter in the K-best method that controls performance and complexity tradeoffs. Consider this optimization problem, the original problem is decomposed into optimally solvable sub-problems. We then formulate this jamming signal design to a non-convex ℓ^p-norm optimization problem with $0 \leq p \leq 1$. It has been shown that such ℓ^p-minimization problem can be effectively solved via an iteratively reweighted algorithm [19], [20], [21], which consists of solving a sequence of weighted ℓ^2-norm minimization problems where the weights used for the next iteration are computed based on the values of the current solution. Finally, we evaluate the proposed technique under practical scenarios with software simulation, in terms of the SU's spectrum sensing results.

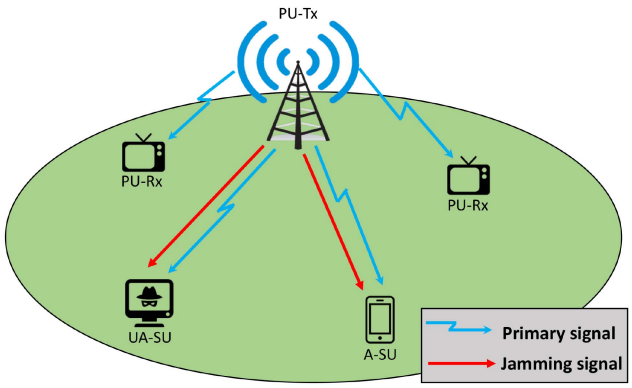

FIGURE 1. System model.

In summary, there are the following contributions presented in this paper.

- We propose an effective sub-optimal approach based on the K-best method to address the jamming signal design of our non-convex QCQP problem at each iteration. The original problem has been decomposed into small sub-problems which can be optimally solved.
- We propose a jamming signal design approach in CR networks with sparse weight representation, which leads to a greener system design. The sparsity is obtained by solving the proposed non-convex ℓ^p-minimization ($0 \leq p \leq 1$) problem with an iterative reweighted approach.
- We then evaluate our approach with practical scenarios simulation. We show that a sparse jamming signal weight can be effectively generated and the A-SUs spectrum sensing performance is well-maintained while UA-SUs' sensing performance is significantly impacted.

This paper is organized as follows. Section II presents the system model and problem formulation. Section III shows the jamming signal design and detailed K-best method. Section IV describes the jamming signal with the general model considered. Section V presents an alternate optimization approach based on the SDR technique. Section VI describes the iteratively reweighted algorithms for sparse jamming signal design. Section VII presents simulation results and related discussions. Finally, conclusions are given in Section VIII.

II. SYSTEM MODEL AND PROBLEM FORMULATION

The proposed SUAC system model in a massive MIMO cognitive radio network is presented in Fig. 1. Each PU is composed of M antennas to serve multiple single-antenna SUs. Assume there are total L SUs with K_{a} A-SUs and K_{ua} UA-SUs ($K_{\mathrm{a}} + K_{\mathrm{ua}} = L$). $\mathbf{h} \in \mathcal{C}^{M\times 1}$ represents the channel link between the PU and SU, $\mathbf{s} \in \mathcal{C}^{M\times 1}$ is the transmitted PU message signal vector, $\mathbf{g} \in \mathcal{C}^{M\times 1}$ denotes the jamming signal sent by the PU, and n denotes the white Gaussian noise with 0 mean and σ^2 variance. $\mathbb{H}_0/\mathbb{H}_1$ denotes PU absent/present status. The jamming signal is only generated when the PU

TABLE 1. List of symbols.

M	PU transmission antenna number
L	Number of SUs
K_{a}	Number of A-SUs
K_{ua}	Number of UA-SUs
K	Number of selected descendants in K-best algorithm
$\mathbb{H}_0/\mathbb{H}_1$	PU's status is absent/present
$\mathbf{g}$	Jamming signal vector sent by PU
$\mathbf{s}$	PU transmission signal vector
r	Received signal at the SU side
n	Additive Gaussian noise
σ^2	Variance of additive noise
$\mathbf{h}$	Channel vector between PU and SU
$\mathbf{h}_{\mathrm{a},i}/\mathbf{h}_{\mathrm{ua},i}$	Channel vector between PU and i^{th} A-SU/UA-SU
$\mathbf{R}_{\mathrm{a},i}/\mathbf{R}_{\mathrm{ua},i}$	Channel covariance matrix of i^{th} A-SU/UA-SU
τ	Scalar to control jamming signal effect on UA-SU
$\mathbf{B}$	$\mathbf{B}=\cap_{i=1}^{K_{\mathrm{a}}}\mathrm{null}\,(\mathbf{R}_{\mathrm{a},i})$ with dimension $M\times S$
$\boldsymbol{\varepsilon}$	Vector satisfies $\mathbf{g}=\mathbf{B}\boldsymbol{\varepsilon}$
$\mathbf{Q}$	Semi-unitary matrix in QR de-composition
$\mathbf{R}$	Upper triangular matrix in QR de-composition
w_i	Weight used in the general model (Approach II)
$\mathbf{H}_{\mathrm{a}}$	$\mathbf{H}_{\mathrm{a}}=[\mathbf{h}_{\mathrm{a},1},\cdots,\mathbf{h}_{\mathrm{a},K_{\mathrm{a}}}]\in\mathcal{C}^{M\times K_{\mathrm{a}}}$
$\mathbf{G}$	A symmetric positive semidefinite matrix with $\mathbf{G}=\mathbf{g}\mathbf{g}^H$
T	Number of randomization trails in SDR algorithm
P	Number of propagation paths in one-ring channel model
χ	Signal wavelength
d	Distance between neighboring antenna elements
α_p	Fading coefficient of p^{th} path
ϵ^2	Variance of α_p
P_{d}	Detection probability
P_{f}	False alarm probability

is absent, and the received signal r at the SU side can be expressed as

$$\begin{cases}\mathbb{H}_0 : r=\mathbf{h}^H\mathbf{g}+n\\ \mathbb{H}_1 : r=\mathbf{h}^H\mathbf{s}+n\end{cases}\tag{1}$$

To further simplify our explanations, the CSI between PU and A-SUs is represented as $\mathbf{H}_{\mathrm{a}}\triangleq[\mathbf{h}_{\mathrm{a},1},\mathbf{h}_{\mathrm{a},2},\ldots,\mathbf{h}_{\mathrm{a},K_{\mathrm{a}}}]\in\mathcal{C}^{M\times K_{\mathrm{a}}}$, where $\mathbf{h}_{\mathrm{a},i}\in\mathcal{C}^{M\times 1}$ represents the channel link between the PU and i^{th} A-SU. The channel link between the primary and UA-SUs is $\mathbf{H}_{\mathrm{ua}}\triangleq[\mathbf{h}_{\mathrm{ua},1},\mathbf{h}_{\mathrm{ua},2},\ldots,\mathbf{h}_{\mathrm{ua},K_{\mathrm{ua}}}]\in\mathcal{C}^{M\times K_{\mathrm{ua}}}$, and $\mathbf{h}_{\mathrm{ua},i}\in\mathcal{C}^{M\times 1}$ represents the channel link between the PU and i^{th} UA-SU. Given $\mathbf{H}_{\mathrm{a}}$ and $\mathbf{H}_{\mathrm{ua}}$, the PU plans to generate jamming signal $\mathbf{g}$ to minimize $\mathbf{g}^H\mathbf{h}_{\mathrm{a},i}$ and simultaneously maximize $\mathbf{g}^H\mathbf{h}_{\mathrm{ua},i}$. In the following sections, we present K-best method based algorithms to create the jammer. For convenience, we present some of the mathematical symbols used in this paper in Table 1.

III. APPROACH I: JAMMING SIGNAL DESIGN

We formulate designing the jamming signal problem as

$$\begin{aligned}\min_{\mathbf{g}\in\mathcal{C}^{M\times 1}}\quad & \|\mathbf{g}\|^2\\ \text{s.t.}\quad & \mathbf{g}^H\mathbf{R}_{\mathrm{a},i}\mathbf{g}=0,\quad i=1,\ldots,K_{\mathrm{a}}\\ & \mathbf{g}^H\mathbf{R}_{\mathrm{ua},j}\mathbf{g}\geq\tau,\ j=1,\ldots,K_{\mathrm{ua}}\end{aligned}\tag{2}$$

where $\mathbf{R}_{\mathrm{a},i}=\mathbf{h}_{\mathrm{a},i}\mathbf{h}_{\mathrm{a},i}^H\in\mathcal{C}^{M\times M}(i=1,\ldots,K_{\mathrm{a}})$ denotes the covariance of i^{th} A-SU. $\mathbf{R}_{\mathrm{ua},j}=\mathbf{h}_{\mathrm{ua},j}\mathbf{h}_{\mathrm{ua},j}^H\in\mathcal{C}^{M\times M}(j=1,\ldots,K_{\mathrm{ua}})$ denotes the covariance matrix of j^{th} UA-SU. τ is a large-magnitude scalar. We start by noting that the first constraint can be eliminated if the jamming vector $\mathbf{g}$ is in the null space of A-SU's corresponding channel covariance matrix $\mathbf{R}_{\mathrm{a},i}$. Let us define $\mathbf{g}=\mathbf{B}\boldsymbol{\varepsilon}$, where $\mathbf{B}=\cap_{i=1}^{K_{\mathrm{a}}}\mathrm{null}(\mathbf{R}_{\mathrm{a},i})$ is the intersection of vector space $\mathrm{null}(\mathbf{R}_{\mathrm{a},i})$ with dimension $\mathbf{B}\in\mathcal{C}^{M\times S}(0<S\leq M)$ and satisfies $\mathbf{B}^H\mathbf{B}=\mathbf{I}$. The objective of (2) can be expressed as

$$\|\mathbf{g}\|^2=\|\mathbf{B}\boldsymbol{\varepsilon}\|^2=\|\boldsymbol{\varepsilon}\|^2\tag{3}$$

and the first constraint in (2) is eliminated since $\mathbf{B}^H\mathbf{R}_{\mathrm{a},i}=\mathbf{0}$, and we always have $\mathbf{g}^H\mathbf{R}_{\mathrm{a},i}\mathbf{g}=\boldsymbol{\varepsilon}^H\mathbf{B}^H\mathbf{R}_{\mathrm{a},i}\mathbf{B}\boldsymbol{\varepsilon}=0$.

The second constraint of (2) can be further written as

$$\mathbf{g}^H\mathbf{R}_{\mathrm{ua},j}\mathbf{g}=\boldsymbol{\varepsilon}^H\mathbf{B}^H\mathbf{R}_{\mathrm{ua},j}\mathbf{B}\boldsymbol{\varepsilon}=\|\mathbf{h}_{\mathrm{ua},j}^H\mathbf{B}\boldsymbol{\varepsilon}\|^2\tag{4}$$

We can now equivalently express problem (2) as

$$\min_{\boldsymbol{\varepsilon}\in\mathcal{C}^{S\times 1}}\ \|\boldsymbol{\varepsilon}\|^2\quad\text{s.t. }\|\mathbf{h}_{\mathrm{ua},j}^H\mathbf{B}\boldsymbol{\varepsilon}\|^2\geq\tau,\quad j=1,\ldots,K_{\mathrm{ua}}\tag{5}$$

Given $\mathbf{C}'=\mathbf{B}^H[\mathbf{h}_{\mathrm{ua},1},\ldots,\mathbf{h}_{\mathrm{ua},K_{\mathrm{ua}}}]\mathrm{diag}\{1/\sqrt{\tau},\ldots,1/\sqrt{\tau}\}$ with dimension $S\times K_{\mathrm{ua}}$, we provide the following proposition.

Proposition 1: Any optimal solution of problem (5) must lie in Range($\mathbf{C}'$).

Proof: We first provide the following QR de-compositions

$$\mathbf{C}'=\mathbf{Q}\mathbf{R}\tag{6}$$

where $\mathbf{Q}$ is a semi-unitary matrix whenever it is non-zero, and $\mathbf{R}=[r_{i,j}]$ is an upper triangular matrix. Any candidate solutions can be represented as $\boldsymbol{\varepsilon}=\mathbf{Q}\boldsymbol{\beta}+\tilde{\mathbf{Q}}\tilde{\boldsymbol{\beta}}$ without loss of generality, where Range($\mathbf{Q}$) $\cup$ Range($\tilde{\mathbf{Q}}$) spans the whole space, $\mathbf{Q}^H\mathbf{Q}=\mathbf{I}\,\&\,\tilde{\mathbf{Q}}^H\mathbf{Q}=\mathbf{0}$. Consider the constraint in (5)

$$\mathbf{h}_{\mathrm{ua},j}^H\mathbf{B}\boldsymbol{\varepsilon}=\mathbf{h}_{\mathrm{ua},j}^H\mathbf{B}\left(\mathbf{Q}\boldsymbol{\beta}+\tilde{\mathbf{Q}}\tilde{\boldsymbol{\beta}}\right)=\mathbf{h}_{\mathrm{ua},j}^H\mathbf{B}\mathbf{Q}\boldsymbol{\beta}+\mathbf{h}_{\mathrm{ua},j}^H\mathbf{B}\tilde{\mathbf{Q}}\tilde{\boldsymbol{\beta}}\tag{7}$$

where $\mathbf{h}_{\mathrm{ua},j}^H\mathbf{B}\mathbf{Q}\boldsymbol{\beta}=\sqrt{\tau}\sum_{i=1}^{j}r_{i,j}^*\beta_i$, and $\mathbf{h}_{\mathrm{ua},j}^H\mathbf{B}\tilde{\mathbf{Q}}\tilde{\boldsymbol{\beta}}=0$. We provide the detailed derivations of Eq. (7) in Appendix A, and we have

$$\mathbf{h}_{\mathrm{ua},j}^H\mathbf{B}\boldsymbol{\varepsilon}=\sqrt{\tau}\sum_{i=1}^{j}r_{i,j}^*\beta_i\tag{8}$$

The objective in problem (5) can be further written as

$$\begin{aligned}\|\boldsymbol{\varepsilon}\|^2&=\|\mathbf{Q}\boldsymbol{\beta}+\tilde{\mathbf{Q}}\tilde{\boldsymbol{\beta}}\|^2\\&=\left(\mathbf{Q}\boldsymbol{\beta}+\tilde{\mathbf{Q}}\tilde{\boldsymbol{\beta}}\right)^H\left(\mathbf{Q}\boldsymbol{\beta}+\tilde{\mathbf{Q}}\tilde{\boldsymbol{\beta}}\right)\\&=\boldsymbol{\beta}^H\mathbf{Q}^H\mathbf{Q}\boldsymbol{\beta}+\boldsymbol{\beta}^H\mathbf{Q}^H\tilde{\mathbf{Q}}\tilde{\boldsymbol{\beta}}+\tilde{\boldsymbol{\beta}}^H\tilde{\mathbf{Q}}^H\mathbf{Q}\boldsymbol{\beta}+\tilde{\boldsymbol{\beta}}^H\tilde{\mathbf{Q}}^H\tilde{\mathbf{Q}}\tilde{\boldsymbol{\beta}}\\&=\|\boldsymbol{\beta}\|^2+\|\tilde{\boldsymbol{\beta}}\|^2\end{aligned}\tag{9}$$

From (8) we can infer that none of the constraints depend on $\tilde{\boldsymbol{\beta}}$, it is optimal to set $\tilde{\boldsymbol{\beta}}$ equals to zero. ■

Define Π as a $K_{\mathrm{ua}}\times K_{\mathrm{ua}}$ permutation matrix and $\mathbf{C}=\mathbf{C}'\Pi$. Specify a QR de-composition $\mathbf{C}=\mathbf{Q}\mathbf{R}$, where $\mathbf{R}$ is a $K_{\mathrm{ua}}\times K_{\mathrm{ua}}$ upper triangular matrix with non-negative diagonal

elements. $\mathbf{Q}$ is an $S \times K_{\text{ua}}$ matrix that contains a zero-column corresponding to each diagonal element of $\mathbf{R}$ that is zero. With **Proposition 1** in hand, we can expand the jamming signal vector we seek as $\boldsymbol{\varepsilon} = \mathbf{Q}\boldsymbol{\beta}$. From (8) and (9), problem (5) can be rewritten as

$$\min_{\boldsymbol{\beta} \in \mathcal{C}^{K_{\text{ua}} \times 1}} \|\boldsymbol{\beta}\|^2 \quad \text{s.t.} \left| \sum_{i=1}^{j} r^*_{i,j} \beta_i \right|^2 \geq 1, \, j = 1, \ldots, K_{\text{ua}} \quad (10)$$

A. K-BEST ALGORITHM

In this section, we present the detailed steps of the proposed K-best algorithm, where K is a tunable parameter ($1 \leq K \leq K_{\text{ua}}$). We present the steps of the K-best algorithm in the following paragraphs.

• *Step 1:* There are K_{ua} selection choices and each choice corresponded descendant is one column from matrix $\mathbf{C}'$. Through two-step sub-problems solving which is described in the following sections, we compute each descendant's metrics and sort the metric's value in ascending order. By selecting the K smallest values, we keep their descendants in the first step.

• *Step j($2 \leq j \leq K_{ua} - 1$):* We expand each K survivor from the $j-1$ step by considering all possibilities that are not been selected in previous steps. Thus, each survivor will be expanded with a new column from matrix $\mathbf{C}'$ that corresponds to the newly selected descendant. In step j, there are K survivors and each survivor with $K_{\text{ua}} - j + 1$ descendants. There are $(K_{\text{ua}} - j + 1)K$ updated optimization sub-problems that need to be solved in this step. Given the calculated value, we sort the metrics in descending order and choose those K lowest values corresponding to descendants in this step.

• *Step K_{ua} (last step):* There is only one remaining descendant for each one of the K remaining nodes from the previous $K_{\text{ua}} - 1$ steps. There are K expanded optimization sub-problems in the last step. By solving those sub-problems and sorting the value from low to high, the final survivor will be selected as the descendant with the smallest value.

Fig. 2 shows a K-best algorithm diagram where there are 5 steps in this example, and we keep $K = 2$ descendants in each of the first $K_{\text{ua}} - 1$ steps. For instance, after calculating all 5 sub-problems in step 1, we sort the calculated metrics from low to high and keep the user 2 and 4 as the survivors. In the last step, the descendant with the minimum metrics will be selected and the selected path is $4 \rightarrow 3 \rightarrow 2 \rightarrow 1 \rightarrow 5$.

B. SUCCESSIVE STEP

In j^{th} step, the associated matrix $\mathbf{C}$ has $j-1$ columns from $\mathbf{C}'$ and we have $\mathbf{C} = \mathbf{QR}$. The computation conducted from this survivor determined vector $\boldsymbol{\beta} = [\beta_1, \ldots, \beta_{j-1}]^T$ such that $\hat{\boldsymbol{\varepsilon}} = \mathbf{Q}\boldsymbol{\beta}$ is a sub-optimal solution to a relaxation of problem (10) which only has constraints corresponding to $j-1$ columns of $\mathbf{C}$. Let $\mathbf{c}'$ denotes any column from the remaining $K_{\text{ua}} - j + 1$ un-selected columns from $\mathbf{C}'$.

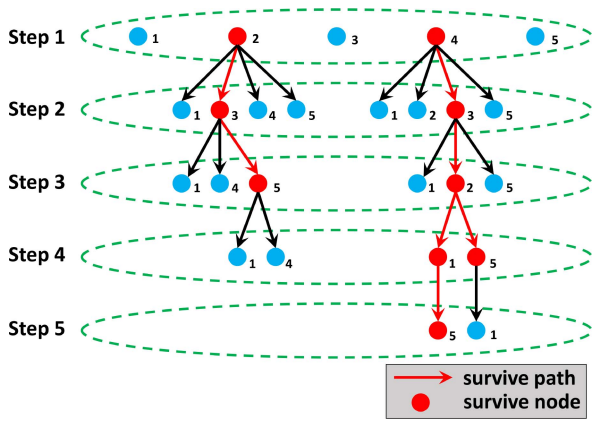

FIGURE 2. Example of K-best algorithm given $K_{\text{ua}} = 5$, $K = 2$. For steps 1 to 4, we keep $K = 2$ descendants (survive paths/nodes highlighted with red color) and the remaining are unselected descendants (blue nodes) and unselected paths (black arrows). In the last step, we only select one survival node.

The updated de-compositions are $[\mathbf{C}, \mathbf{c}'] = \mathbf{Q}'\mathbf{R}'$, with $\mathbf{R}' = [r'_{i,j}]$. Let $\boldsymbol{\beta}' = [\gamma\beta_1, \ldots, \gamma\beta_{j-1}, \beta]^T$ denotes the updated and expanded $\boldsymbol{\beta}$. Notice that γ and β are two complex variables that are determined by solving the following sub-problem.

$$\begin{aligned} \min_{\beta, \gamma \in \mathcal{C}} \quad & |\beta|^2 + \sum_{i=1}^{j-1} \left(|\gamma|^2 |\beta_i|^2 \right) \\ \text{s.t.} \quad & |\gamma| \geq 1 \\ & \left| \left(r'_{j,j}\right)^* \beta + \gamma \sum_{i=1}^{j-1} \left(\left(r'_{i,j}\right)^* \beta_i \right) \right|^2 \geq 1 \end{aligned} \quad (11)$$

Notice that only the last constraint depends on the phases of β and γ, the other constraint and the objective function are invariant to the phases. Without loss of optimality, we can suppose that the phase of β equals to the phase of $r'_{j,j}$, and the phase of γ equals the phase of $\sum_{i=1}^{j-1}(r'_{i,j}\beta_i^*)$. Thus, define $\tilde{\beta} = |\beta|$ and $\tilde{\gamma} = |\gamma|$. Problem (11) can be expressed as

$$\begin{aligned} \min_{\tilde{\beta}, \tilde{\gamma} \in \mathcal{R}_{\geq 0}} \quad & \tilde{\beta}^2 + \tilde{\gamma}^2 \sum_{i=1}^{j-1} |\beta_i|^2 \\ \text{s.t.} \quad & \tilde{\gamma} \geq 1 \\ & \left| r'_{j,j} \right| \tilde{\beta} + \tilde{\gamma} \left| \sum_{i=1}^{j-1} \left(\left(r'_{i,j}\right)^* \beta_i \right) \right| \geq 1 \end{aligned} \quad (12)$$

where we have a convex quadratic objective and convex constraint conditions. We can explicitly solve this optimization problem through Karush-Kuhn-Tucker (KKT) conditions. We start by noting that either $\sum_{i=1}^{j-1} |\beta_i|^2 = 0$, $|r'_{j,j}| = 0$ or $|\sum_{i=1}^{j-1}((r'_{i,j})^*\beta_i)| = 0$, the optimal solution can be easily obtained. If $\sum_{i=1}^{j-1} |\beta_i|^2 > 0$, $|r'_{j,j}| > 0$, and $|\sum_{i=1}^{j-1}((r'_{i,j})^*\beta_i)| > 0$, we provide following proposition. Detailed proof can be found in Appendix B.

Proposition 2: When $\sum_{i=1}^{j-1}|\beta_i|^2 > 0$, $|r'_{j,j}| > 0$, and $|\sum_{i=1}^{j-1}((r'_{i,j})^*\beta_i)| > 0$, optimal solution of problem (12) is given as follows:

- $\tilde{\beta}_{\text{opt}} = 0, \tilde{\gamma}_{\text{opt}} = 1$, if $|\sum_{i=1}^{j-1}((r'_{i,j})^*\beta_i)| \geq 1$;
- $\tilde{\beta}_{\text{opt}} = \frac{1-|\sum_{i=1}^{j-1}((r'_{i,j})^*\beta_i)|}{|r'_{j,j}|}, \tilde{\gamma}_{\text{opt}} = 1$,

tif $|\sum_{i=1}^{j-1}((r'_{i,j})^*\beta_i)| < 1$ tand $\sum_{i=1}^{j-1}|\beta_i|^2|r'_{j,j}|^2 + |\sum_{i=1}^{j-1}((r'_{i,j})^*\beta_i)|^2 - |\sum_{i=1}^{j-1}((r'_{i,j})^*\beta_i)| > 0$;

- $\tilde{\beta}_{\text{opt}} = \frac{|r'_{j,j}|\sum_{i=1}^{j-1}|\beta_i|^2}{\sum_{i=1}^{j-1}|\beta_i|^2|r'_{j,j}|^2+|\sum_{i=1}^{j-1}((r'_{i,j})^*\beta_i)|^2}$,

$\tilde{\gamma}_{\text{opt}} = \frac{|\sum_{i=1}^{j-1}((r'_{i,j})^*\beta_i)|}{\sum_{i=1}^{j-1}|\beta_i|^2|r'_{j,j}|^2+|\sum_{i=1}^{j-1}((r'_{i,j})^*\beta_i)|^2}$,

if $|\sum_{i=1}^{j-1}((r'_{i,j})^*\beta_i)| < 1$ and $\sum_{i=1}^{j-1}|\beta_i|^2|r'_{j,j}|^2 + |\sum_{i=1}^{j-1}((r'_{i,j})^*\beta_i)|^2 - |\sum_{i=1}^{j-1}((r'_{i,j})^*\beta_i)| \leq 0$.

IV. APPROACH II: GENERAL MODEL

In previous Approach I analysis, jamming vector $\mathbf{g}$ is calculated by maximizing impact on UA-SUs ($\mathbf{g}^H\mathbf{R}_{\text{ua}}\mathbf{g} \geq \tau$) and minimizing the influence on A-SUs ($\mathbf{g}^H\mathbf{R}_{\text{a}}\mathbf{g} = 0$). However, under the condition that A-SUs channel vector $\mathbf{h}_{\text{a}}$ and UA-SUs channel vector $\mathbf{h}_{\text{ua}}$ are highly correlated, it will be challenging to obtain $\mathbf{g}$ satisfies the constraints shown in Approach I at the same time. To address this issue, consider the following problem,

$$\begin{aligned}\min_{\mathbf{g}\in\mathcal{C}^{M\times 1}} \quad & w_0\|\mathbf{g}\|^2 + \sum_{i=1}^{K_{\text{a}}} w_i\|\mathbf{h}_{\text{a},i}^H\mathbf{g}\|^2 \\ \text{s.t.} \quad & \|\mathbf{h}_{\text{ua},j}^H\mathbf{g}\|^2 \geq \tau,\ j = 1,\ldots,K_{\text{ua}}\end{aligned} \tag{13}$$

where $w_i \in \mathcal{R}^+ (i = 0, 1, \ldots, K_{\text{a}})$ are given weights. Specifically, if we want to find a jamming signal $\mathbf{g}$ has a negligible effect on A-SUs, we could change $w_i (i = 1, 2, \ldots, K_{\text{a}})$ to be a large value, in order to force the jamming signal within the desired subspace. Define a matrix $\mathbf{C}' = [\mathbf{h}_{\text{ua},1}, \ldots, \mathbf{h}_{\text{ua},K_{\text{ua}}}]\text{diag}\{1/\sqrt{\tau}, \ldots, 1/\sqrt{\tau}\} \in \mathcal{C}^{M\times K_{\text{ua}}}$, and a matrix $\mathbf{H}_{\text{a}} = [\mathbf{h}_{\text{a},1}, \ldots, \mathbf{h}_{\text{a},K_{\text{a}}}] \in \mathcal{C}^{M\times K_{\text{a}}}$. Consider following QR de-composition

$$[\mathbf{C}', \mathbf{H}_{\text{a}}] = \mathbf{QR} \tag{14}$$

where $\mathbf{Q}$ is a semi-unitary matrix whenever it is non-zero, and $\mathbf{R} = [r_{i,j}]$ is an upper triangular. Suppose any candidate solutions for problem (13) can be represented as $\mathbf{g} = \mathbf{Q}\boldsymbol{\beta} + \tilde{\mathbf{Q}}\tilde{\boldsymbol{\beta}}$, where Range($\mathbf{Q}$) $\cup$ Range($\tilde{\mathbf{Q}}$) spans the whole space, $\mathbf{Q}^H\mathbf{Q} = \mathbf{I}\,\&\,\tilde{\mathbf{Q}}^H\mathbf{Q} = \mathbf{0}$. We extend **Proposition 1** to obtain the following **Proposition 3**. The detailed proof can be found in Appendix C.

Proposition 3: Any optimal solution of problem (13) must lie in Range($[\mathbf{C}', \mathbf{H}_{\text{a}}]$).

From (60) we have $\mathbf{h}_{\text{a},i}^H\tilde{\mathbf{Q}}\tilde{\boldsymbol{\beta}} = 0$. We then rewrite the objective function in problem (13) as follows

$$\begin{aligned} & w_0\|\mathbf{g}\|^2 + \sum_{i=1}^{K_{\text{a}}} w_i\|\mathbf{h}_{\text{a},i}^H\mathbf{g}\|^2 \\ &= w_0\|\mathbf{Q}\boldsymbol{\beta} + \tilde{\mathbf{Q}}\tilde{\boldsymbol{\beta}}\|^2 + \sum_{i=1}^{K_{\text{a}}} w_i\left\|\mathbf{h}_{\text{a},i}^H\left(\mathbf{Q}\boldsymbol{\beta} + \tilde{\mathbf{Q}}\tilde{\boldsymbol{\beta}}\right)\right\|^2 \\ &= w_0\|\boldsymbol{\beta}\|^2 + w_0\|\tilde{\boldsymbol{\beta}}\|^2 + \sum_{i=1}^{K_{\text{a}}} w_i\|\mathbf{h}_{\text{a},i}^H\mathbf{Q}\boldsymbol{\beta}\|^2 \end{aligned} \tag{15}$$

From **Proposition 3**, we can further simplify the objective by setting $\tilde{\boldsymbol{\beta}}$ to zero. Problem (13) can be expressed as

$$\begin{aligned}\min_{\boldsymbol{\beta}\in\mathcal{C}^{L\times 1}} \quad & w_0\|\boldsymbol{\beta}\|^2 + \sum_{i=1}^{K_{\text{a}}} w_i\left|\sum_{k=1}^{K_{\text{ua}}+i} r^*_{k,K_{\text{ua}}+i}\beta_k\right|^2 \\ \text{s.t.} \quad & \left|\sum_{k=1}^{j} r^*_{k,j}\beta_k\right|^2 \geq 1,\ j = 1,\ldots,K_{\text{ua}}\end{aligned} \tag{16}$$

We then present a solution to solve the problem (16) via a sub-problem approach based on the K-best method.

A. SUCCESSIVE STEP

In j^{th} step, assume the associated matrix $\mathbf{C}$ has $j-1$ columns from $\mathbf{C}'$. The computation conducted from this survivor determined vector $\boldsymbol{\beta}' = [\beta_1, \ldots, \beta_{j-1}, \hat{\beta}_1, \ldots, \hat{\beta}_{K_{\text{a}}}]^T$. Let $\mathbf{c}$ denotes any column from the remaining $K_{\text{ua}} - j + 1$ un-selected columns from $\mathbf{C}'$. The updated decompositions are $[\mathbf{C}, \mathbf{c}, \mathbf{H}_{\text{a}}] = \mathbf{QR}$, with $\mathbf{R} = [r_{i,j}]$. Let $\boldsymbol{\beta} = [\gamma\beta_1, \ldots, \gamma\beta_{j-1}, \beta, \tilde{\beta}_1, \ldots, \tilde{\beta}_{K_{\text{a}}}]^T$ denotes the updated and expanded $\boldsymbol{\beta}'$. Here $\gamma, \beta, \tilde{\beta}_1, \ldots, \tilde{\beta}_{K_{\text{a}}}$ are $K_{\text{a}} + 2$ variables that are determined by solving following optimization problem

$$\begin{aligned}\min_{\gamma,\beta,\tilde{\beta}_1,\ldots,\tilde{\beta}_{K_{\text{a}}}\in\mathcal{C}} \quad & w_0|\beta|^2 + w_0\sum_{i=1}^{j-1}|\gamma\beta_i|^2 + w_0\sum_{i=1}^{K_{\text{a}}}\left|\tilde{\beta}_i\right|^2 \\ & + \sum_{i=1}^{K_{\text{a}}} w_i\left|r^*_{j,j+i}\beta + \sum_{k=1}^{j-1} r^*_{k,j+i}\gamma\beta_k + \sum_{k=1}^{i} r^*_{j+k,j+i}\tilde{\beta}_k\right|^2 \\ \text{s.t.} \quad & |\gamma|^2 \geq 1 \\ & \left|r^*_{j,j}\beta + \gamma\sum_{k=1}^{j-1} r^*_{k,j}\beta_k\right|^2 \geq 1\end{aligned} \tag{17}$$

which can be expressed as the following compact form

$$\min_{\mathbf{x}\in\mathcal{C}^{(K_{\text{a}}+2)\times 1}} \mathbf{x}^H\mathbf{D}\mathbf{x} \quad \text{s.t.}\, \mathbf{x}^H\mathbf{v}\mathbf{v}^H\mathbf{x} \geq 1,\ \mathbf{x}^H\mathbf{u}\mathbf{u}^H\mathbf{x} \geq 1 \tag{18}$$

where

$$\begin{aligned} & \mathbf{x} = [\gamma, \beta, \tilde{\beta}_1, \ldots, \tilde{\beta}_{K_{\text{a}}}]^T, \mathbf{u} = \left[1, \underbrace{0, \ldots, 0}_{(K_{\text{a}}+1)\,0'\text{s}}\right]^T, \\ & \mathbf{v} = \left[\sum_{k=1}^{j-1}\left(r_{k,j}\beta_k^*\right), r_{j,j}, \underbrace{0, \ldots, 0}_{K_{\text{a}}\,0'\text{s}}\right]^T, \\ & \mathbf{D} = \text{diag}\left\{w_0\sum_{i=1}^{j-1}\left(|\beta_i|^2\right), \underbrace{w_0, \ldots, w_0}_{(K_{\text{a}}+1)\,w'_0\text{s}}\right\} + \sum_{i=1}^{K_{\text{a}}} w_i\mathbf{Q}_i \end{aligned} \tag{19}$$

$\mathbf{Q}_i \in \mathcal{C}^{(K_a+2)\times(K_a+2)}$ is defined as $\mathbf{Q}_i = \mathbf{q}_i\mathbf{q}_i^H$ with

$$\mathbf{q}_i = \left[\sum_{k=1}^{j-1} r_{k,j+i}\beta_k^*, r_{j,j+i}, r_{j+1,j+i}, \ldots, r_{j+i,j+i}, \underbrace{0, \ldots, 0}_{(K_a-i)\ 0's}\right]^T \tag{20}$$

Denote $\mathbf{y} \triangleq \mathbf{D}^{\frac{1}{2}}\mathbf{x}$ with dimension $\mathbf{y} \in \mathcal{C}^{(K_a+2)\times 1}$, and we then have $\mathbf{x} = \mathbf{D}^{-\frac{1}{2}}\mathbf{y}$. Optimization problem (18) can be rewritten as

$$\min_{\mathbf{y}\in\mathcal{C}^{(K_a+2)\times 1}} \|\mathbf{y}\|^2 \quad \text{s.t.}\ \|\mathbf{v}^H\mathbf{D}^{-\frac{1}{2}}\mathbf{y}\|^2 \geq 1,\ \|\mathbf{u}^H\mathbf{D}^{-\frac{1}{2}}\mathbf{y}\|^2 \geq 1 \tag{21}$$

Define a matrix $\tilde{\mathbf{C}} = [\mathbf{D}^{-\frac{1}{2}}\mathbf{v}, \mathbf{D}^{-\frac{1}{2}}\mathbf{u}] \in \mathcal{C}^{(K_a+2)\times 2}$, and the corresponded QR de-composition is $\tilde{\mathbf{C}} = \mathbf{UL}$, where $\mathbf{U} \in \mathcal{C}^{(K_a+2)\times 2}$ is a semi-unitary matrix satisfies $\mathbf{U}^H\mathbf{U} = \mathbf{I}$ and $\mathbf{L} \in \mathcal{C}^{2\times 2}$ is an upper triangular matrix which can be represented as

$$\mathbf{L} = \begin{pmatrix} l_{1,1} & l_{1,2} \\ 0 & l_{2,2} \end{pmatrix},\ l_{1,1}, l_{2,2} > 0 \tag{22}$$

Without loss of optimality, denote $\mathbf{y} = \mathbf{U}[\nu, \zeta]^T$, the new formulation can be expressed as

$$\min_{\nu,\zeta\in\mathcal{C}} |\nu|^2 + |\zeta|^2 \quad \text{s.t.}\ \left|l_{1,1}\nu\right|^2 \geq 1,\ \left|l_{1,2}^*\nu + l_{2,2}\zeta\right|^2 \geq 1 \tag{23}$$

Notice that only the last constraint depends on the phase of ν whereas the other constraint and the objective function are invariant to them. Thus, we can suppose that the phase of ν equals to the phase of $l_{1,2}$. Suppose $|\nu| = (\tilde{a} + \tilde{b})$ with $\tilde{a} = \frac{1}{l_{1,1}}$, and $|\zeta| = \tilde{c}$, problem (23) is equivalent to

$$\min_{\tilde{b},\tilde{c}\in\mathcal{R}^+} \left(\tilde{a}+\tilde{b}\right)^2 + \tilde{c}^2 \quad \text{s.t.}\ \tilde{a} = \frac{1}{l_{1,1}},\ |l_{1,2}|\left(\tilde{a}+\tilde{b}\right) + \tilde{c}l_{2,2} \geq 1 \tag{24}$$

such formulation is a convex optimization problem and can be solved in closed form, which is provided in the following **Proposition 4**.

Proposition 4: Any optimal solution of problem (23) is given as follows:

- $\nu_{\text{opt}} = \frac{1}{l_{1,1}}\frac{l_{1,2}}{|l_{1,2}|}$, $\zeta_{\text{opt}} = 0$, *if* $1 - \frac{|l_{1,2}|}{l_{1,1}} \leq 0$;
- $\nu_{\text{opt}} = \frac{l_{1,2}}{l_{2,2}^2+|l_{1,2}|^2}$, $\zeta_{\text{opt}} = \frac{l_{2,2}}{l_{2,2}^2+|l_{1,2}|^2}$, if $1 - \frac{|l_{1,2}|}{l_{1,1}} > 0$ and $l_{1,1}|l_{1,2}| > |l_{1,2}|^2 + l_{2,2}^2$;
- $\nu_{\text{opt}} = \frac{l_{1,2}}{l_{1,1}|l_{1,2}|}$, $\zeta_{\text{opt}} = \frac{l_{1,1}-|l_{1,2}|}{l_{1,1}l_{2,2}}$, if $1 - \frac{|l_{1,2}|}{l_{1,1}} > 0$ and $l_{1,1}|l_{1,2}| \leq |l_{1,2}|^2 + l_{2,2}^2$;

Proof: Denote $\Xi = 1 - \tilde{a}|l_{1,2}| = 1 - \frac{|l_{1,2}|}{l_{1,1}}$.

Case I: $\Xi \leq 0$.

Here $\tilde{b}_{\text{opt}} = \tilde{c}_{\text{opt}} = 0$. Thus, $\nu_{\text{opt}} = \frac{1}{l_{1,1}}\frac{l_{1,2}}{|l_{1,2}|}$ and $\zeta_{\text{opt}} = 0$. When $\Xi > 0$, the optimal solution is obtained by investigating relationships between the circle, $(\tilde{b} + \frac{1}{l_{1,1}})^2 + \tilde{c}^2 = C$, and the line, $|l_{1,2}|\tilde{b} + l_{2,2}\tilde{c} = \Xi$. Specifically, the line is tangential to the circle at the point denoted as S. In Fig. 3, the optimal solution is marked by a red dot. As shown in Fig. 3 (left), the tangent point S is the optimal solution if S is located in the first quadrant. Otherwise, the optimal solution is obtained at the intersection point (shown in Fig. 3 (right)) of the straight line and the vertical axis ($\tilde{c}$-axis).

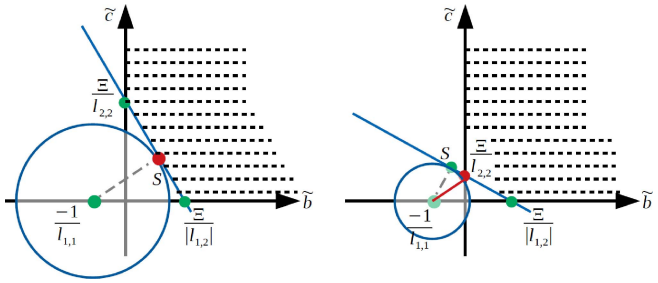

FIGURE 3. Sketch both the objective function (circle) and the constraint function (straight line) of the optimization problem (24) on a 2-D plane ($\tilde{b}$-$\tilde{c}$ plane). The shadowing area (dashed lines) denotes the set of feasible solutions. **Left:** The tangent point *S* located on the first quadrant, the optimal solution is obtained at this tangent point (red dot); **Right:** The tangent point *S* is located on the second quadrant, the optimal solution is obtained at the intersection point (red dot) of the straight line and the $\tilde{c}$-axis.

Denote the coordinate of point S as $(S_{\tilde{b}}, S_{\tilde{c}})$, and after solving the following two equations,

$$\begin{aligned} \frac{S_{\tilde{c}}}{S_{\tilde{b}} + \frac{1}{l_{1,1}}} &= -\frac{-\frac{\Xi}{|l_{1,2}|}}{\frac{\Xi}{l_{2,2}}} \\ |l_{1,2}|S_{\tilde{b}} + l_{2,2}S_{\tilde{c}} &= \Xi \end{aligned} \tag{25}$$

we have $S_{\tilde{b}} = \frac{l_{1,1}|l_{1,2}|-|l_{1,2}|^2-l_{2,2}^2}{l_{1,1}l_{2,2}^2+l_{1,1}|l_{1,2}|^2}$ and $S_{\tilde{c}} = \frac{l_{2,2}}{l_{2,2}^2+|l_{1,2}|^2}$.

Case II: $\Xi > 0$ and $l_{1,1}|l_{1,2}| > |l_{1,2}|^2 + l_{2,2}^2$.

When the tangent point S located on the first quadrant (Fig. 3 (left)), $S_{\tilde{b}} > 0$ and we have $l_{1,1}|l_{1,2}| > |l_{1,2}|^2 + l_{2,2}^2$. $\tilde{b}_{\text{opt}} = S_{\tilde{b}} = \frac{l_{1,1}|l_{1,2}|-|l_{1,2}|^2-l_{2,2}^2}{l_{1,1}l_{2,2}^2+l_{1,1}|l_{1,2}|^2}$, and $\tilde{c}_{\text{opt}} = S_{\tilde{c}} = \frac{l_{2,2}}{l_{2,2}^2+|l_{1,2}|^2}$. Thus, we have

$$\begin{aligned} \nu_{\text{opt}} &= \left(\frac{l_{1,1}|l_{1,2}| - |l_{1,2}|^2 - l_{2,2}^2}{l_{1,1}l_{2,2}^2 + l_{1,1}|l_{1,2}|^2} + \frac{1}{l_{1,1}}\right)\frac{l_{1,2}}{|l_{1,2}|} \\ &= \frac{l_{1,2}}{l_{2,2}^2 + |l_{1,2}|^2} \end{aligned} \tag{26}$$

and $\zeta_{\text{opt}} = \frac{l_{2,2}}{l_{2,2}^2+|l_{1,2}|^2}$.

Case III: $\Xi > 0$ and $l_{1,1}|l_{1,2}| \leq |l_{1,2}|^2 + l_{2,2}^2$. Consider the scenario shows in Fig. 3 (right) and we have $S_{\tilde{b}} \leq 0$, which leads the condition $l_{1,1}|l_{1,2}| \leq |l_{1,2}|^2 + l_{2,2}^2$. The optimal solution is obtained at the intersection point $(0, \frac{\Xi}{l_{2,2}})$ and we have $\tilde{b}_{\text{opt}} = 0$, $\tilde{c}_{\text{opt}} = \frac{\Xi}{l_{2,2}} = \frac{l_{1,1}-|l_{1,2}|}{l_{1,1}l_{2,2}}$. Then we have $\nu_{\text{opt}} = \frac{l_{1,2}}{l_{1,1}|l_{1,2}|}$ and $\zeta_{\text{opt}} = \frac{l_{1,1}-|l_{1,2}|}{l_{1,1}l_{2,2}}$. ■

V. ALTERNATE METHOD

In this section, we briefly show an alternative jamming signal design method based on the semidefinite relaxation (SDR) [10] technique, which has been discussed in [9].

Consider the constraint problem shown in Eq. (2), which we have rewritten as follows

$$\begin{aligned}\min_{\mathbf{g}\in\mathcal{C}^{M\times 1}} \quad & \|\mathbf{g}\|^2 \\ \text{s.t.} \quad & \mathbf{g}^H\mathbf{R}_{\mathrm{a},i}\mathbf{g}=0, \quad i=1,\ldots,K_{\mathrm{a}} \\ & \mathbf{g}^H\mathbf{R}_{\mathrm{ua},j}\mathbf{g}\geq\tau,\ j=1,\ldots,K_{\mathrm{ua}}\end{aligned} \tag{27}$$

Such QCQP problem can be solved via the semidefinite relaxation approach. Denote $\mathbf{G}=\mathbf{g}\mathbf{g}^H$, and $\mathbf{G}$ is a positive symmetric semidefinite matrix. Without considering the rank of matrix $\mathbf{G}$ equals to one, the problem of (27) can be represented as

$$\begin{aligned}\min_{\mathbf{G}\in\mathcal{H}^{M\times 1}} \quad & \mathrm{Tr}(\mathbf{G}) \\ \text{s.t.} \quad & \mathrm{Tr}\big(\mathbf{R}_{\mathrm{a},i}\mathbf{G}\big)=0, \quad i=1,\ldots,K_{\mathrm{a}} \\ & \mathrm{Tr}\big(\mathbf{R}_{\mathrm{ua},j}\mathbf{G}\big)\geq\tau, \quad j=1,\ldots,K_{\mathrm{ua}} \\ & \mathbf{G}\succeq\mathbf{0}\end{aligned} \tag{28}$$

where $\mathcal{H}^{M\times 1}$ denotes the set of $M\times M$ complex Hermitian matrices. $\boldsymbol{\psi}_t$ is a vector randomly distributed with $\boldsymbol{\psi}_t\sim\mathcal{CN}(\mathbf{0},\mathbf{G}^*)$, $t=1,\ldots,T$, where T denotes the randomization trials number. Consider each trail (say t^{th} trail), we obtain the feasible solution $\mathbf{g}_t(\boldsymbol{\psi})=\frac{\sqrt{\tau}\boldsymbol{\psi}_t}{\sqrt{\min_{j=1,\ldots,K_{\mathrm{ua}}}\boldsymbol{\psi}_t^H\mathbf{R}_{\mathrm{ua},j}\boldsymbol{\psi}_t}}$. The best solution after T trails can be determined by solving the problem $\mathbf{g}^*=\arg\min_{\mathbf{g}_t(\boldsymbol{\psi})}\mathbf{g}_t(\boldsymbol{\psi})^H\mathbf{g}_t(\boldsymbol{\psi})$. The worst-case computation complexity of the SDR problem (28) is $\mathcal{O}(\max\{L,M\}^4M^{1/2}\log(1/\delta))$ [10], where $\delta>0$ is a given solution accuracy.

VI. ITERATIVELY REWEIGHTED ALGORITHMS FOR SPARSE JAMMING SIGNAL DESIGN

From the perspective of a jammer in the cognitive radio network, the jammer intends to generate a jamming signal with a sparse configuration in order to mitigate the influence added to the CR network. To design a sparse jamming signal, instead of formulating a ℓ^0 optimization problem (NP-hard), we consider ℓ^1 optimization as an approximation solution. In addition, it was shown empirically that using ℓ^p with $p<1$ can obtain more sparse results than with $p=1$ [19]. In this research, we plan to consider ℓ^p-norm optimization problem with $p\in[0,1]$ in the jamming signal $\mathbf{g}$ design. In particular, similar to the problem shown in (13), we re-design our problem in the following format:

$$\begin{aligned}\min_{\mathbf{g}\in\mathcal{C}^{M\times 1}} \quad & w_0\|\mathbf{g}\|^p+\sum_{i=1}^{K_{\mathrm{a}}}w_i\|\mathbf{h}_{\mathrm{a},i}^H\mathbf{g}\|^2 \\ \text{s.t.} \quad & \|\mathbf{h}_{\mathrm{ua},j}^H\mathbf{g}\|^2\geq\tau,\ j=1,\ldots,K_{\mathrm{ua}}\end{aligned} \tag{29}$$

where the objective function is a ℓ^p-norm of the jamming signal $\mathbf{g}$, with $0\leq p\leq 1$. Early papers considered iteratively reweighted algorithms for solving this $\ell^p(0\leq p\leq 1)$ norm optimization problem [20], specifically, we replace the ℓ^p objective function in (29) by a weighted ℓ^2-norm $\|\mathbf{g}\|^p=\sum_{k=1}^M\alpha_k g_k^*g_k$, where g_k represents the k^{th} component in vector $\mathbf{g}$, and weights α_k are computed from the previous iterate $\mathbf{g}^{(t-1)}$. After considering the damping approach, the weight α_k is given as $\alpha_k=(g_k^*g_k+\phi)^{\frac{p}{2}-1}$. The parameter $\phi>0$ is introduced in order to provide stability [21]. Appropriate determination of the value of ϕ is very crucial in order to perform a fast, accurate, and stable algorithm process. Given $\Upsilon=\mathrm{diag}\{\alpha_1,\ldots,\alpha_M\}$, we have $\|\mathbf{g}\|^p=\|\Upsilon^{\frac{1}{2}}\mathbf{g}\|^2$. Problem (29) can now equivalently be expressed as

$$\begin{aligned}\min_{\mathbf{g}\in\mathcal{C}^{M\times 1}} \quad & w_0\|\Upsilon^{\frac{1}{2}}\mathbf{g}\|^2+\sum_{i=1}^{K_{\mathrm{a}}}w_i\|\mathbf{h}_{\mathrm{a},i}^H\mathbf{g}\|^2 \\ \text{s.t.} \quad & \|\mathbf{h}_{\mathrm{ua},j}^H\mathbf{g}\|^2\geq\tau,\ j=1,\ldots,K_{\mathrm{ua}}\end{aligned} \tag{30}$$

The above non-convex optimization problem can be solved via an iterative algorithm that alternates between estimating $\mathbf{g}$ and updating the weight α_k. During each iteration, $\mathbf{g}$ will be calculated using the proposed K-best algorithm. The steps of the algorithm are as follows:

(1). Initialize the iteration number t to zero, determine the parameter ϕ's initial value, and set $\alpha_k^{(0)}=1$, $k=1,\ldots,M$.

(2). Solve the following non-convex QCQP minimization problem via the K-best approach:

$$\begin{aligned}\min_{\mathbf{g}^{(t)}\in\mathcal{C}^{M\times 1}} \quad & w_0\|\Upsilon^{\frac{1}{2}(t)}\mathbf{g}^{(t)}\|^2+\sum_{i=1}^{K_{\mathrm{a}}}w_i\|\mathbf{h}_{\mathrm{a},i}^H\mathbf{g}^{(t)}\|^2 \\ \text{s.t.} \quad & \|\mathbf{h}_{\mathrm{ua},j}^H\mathbf{g}^{(t)}\|^2\geq\tau,\ j=1,\ldots,K_{\mathrm{ua}}\end{aligned} \tag{31}$$

Detailed procedures to solve this problem can be seen in Appendix D.

(3). Update the weights $\alpha_k(k=1,\ldots,M)$: $\alpha_k^{(t+1)}=(g_k^{*(t)}g_k^{(t)}+\phi)^{\frac{p}{2}-1}$.

(4). Increase iteration t and go to step 2, or terminate the algorithm if the convergence condition is satisfied.

Assume there are total T_{r} iterations, the worst-case (i.e., the convergence condition during the iteration never satisfied) computation complexity of the proposed iteratively reweighted algorithm is $\mathcal{O}(T_{\mathrm{r}}K_{\mathrm{ua}}ML^2)$.

VII. SIMULATION RESULTS AND RELATED DISCUSSIONS

In this section, we present the simulation results of the proposed method. We consider a single-cell scenario in which the PU equipped with $M=64$ transmission antennas, communicates with L single antenna-equipped SUs. We adopt the popular one-ring channel model in our simulation, which has been extensively studied to characterize massive MIMO channels [22], [23], [24]. Denote the total number of the propagation paths as P, the channel vector $\mathbf{h}$ can be expressed as $\mathbf{h}=\frac{1}{\sqrt{P}}\sum_{p=1}^P\alpha_p\mathbf{a}(\theta_p)$, where $\alpha_p\sim\mathcal{CN}(0,\epsilon^2)$ denotes the fading coefficient of p^{th} path, and $\mathbf{a}(\theta_p)\triangleq[1\ e^{-j(\frac{2\pi}{\chi})d\cos(\theta_p)}\ \ldots\ e^{-j(M-1)(\frac{2\pi}{\chi})d\cos(\theta_p)}]^T$ is the steering vector, χ represents the signal wavelength, d denotes the distance between neighboring antenna elements, and $\theta_p\in[0,\pi]$ represents the p^{th} path azimuth angle of arrival (AoA). In our simulation, we have $P=100$, $d=\frac{1}{2}\chi$,

and $\epsilon = 1$. The mean angle of i^{th} SU, $\bar{\theta}_i$, is assumed to be uniformly distributed over an interval $[\frac{\pi}{4} - \frac{\pi}{6}, \frac{\pi}{4} + \frac{\pi}{6}]$. Denote the angle of i^{th} SU's p^{th} path as $\theta_{i,p}$, which is assumed uniformly distributed over an interval $[\bar{\theta}_i - \frac{\pi}{10}, \bar{\theta}_i + \frac{\pi}{10}]$. In the following figures, the key simulation results are presented as follows. There are two important measures in cognitive radio: PU detection probability (P_{d}) and false alarm probability (P_{f}). Notice that, P_{f} should be a very small value in order to let SUs find the empty spectrum efficiently, and P_{d} is a large value (i.e., $P_{\text{d}} \geq 90\%$) in system design in order to avoid significant interference to the PUs.

A. PERFORMANCE OF VARIOUS K

In this section, we present the spectrum sensing performance of SUs with various numbers of K considering the K-best optimization algorithm. Number of SUs is $L = 30$, among which there are $K_{\text{a}} = 15$ A-SUs and $K_{\text{ua}} = 15$ UA-SUs.

Fig. 4 shows A-SU and UA-SU's false alarm probability P_{f} versus signal-to-noise ratio (SNR) under the condition that the detection probability is $P_{\text{d}} = 99\%$ consider Approach I. Perfect CSI scenario is considered and $K = 1, 5, 15$. From the simulation results, we have the following observations.

1) For A-SUs with a different number of K, P_{f} performance improves with the increasing SNR values.

2) The spectrum detection performance of UA-SU is significantly degraded by the proposed method (Approach I).

3) For A-SUs, the detection performance with various K is very close.

4) For UA-SUs, the detection performance becomes worse given larger K.

Fig. 5 presents A-SU and UA-SU's P_{f} versus SNR under the condition that $P_{\text{d}} = 99\%$ consider Approach II. $K = 1, 15$, and perfect CSI is considered. We set $w_i = 100 (i = 1, \ldots, K_{\text{a}})$ and $w_0 = 1$ in Eq. (13). From the simulation results we can see that:

1) A-SUs spectrum sensing performance improves with the increasing SNR value and is irrelevant to the K value.

2) UA-SUs spectrum sensing performance was significantly degraded by the proposed Approach II algorithm. A larger K value corresponds to better jamming performance.

B. PERFORMANCE OF VARIOUS W_I IN APPROACH II

In this section, we show the SUs spectrum sensing performance in Approach II with a various number of weights w_i ($w_i = 10, 1000$) in Eq. (13). We consider $K_{\text{a}} = 15$ A-SUs and $K_{\text{ua}} = 15$ UA-SUs in our simulation. Fig. 6 shows A-SU and UA-SU's P_{f} versus SNR given $P_{\text{d}} = 99\%$, $K = 5$, and perfect CSI. We have the following observations from the simulation results.

1) For A-SUs, larger weight w_i value ($w_i = 1000$) shows better spectrum sensing performance.

2) For UA-SUs, smaller weight w_i value ($w_i = 10$) have a better jamming performance.

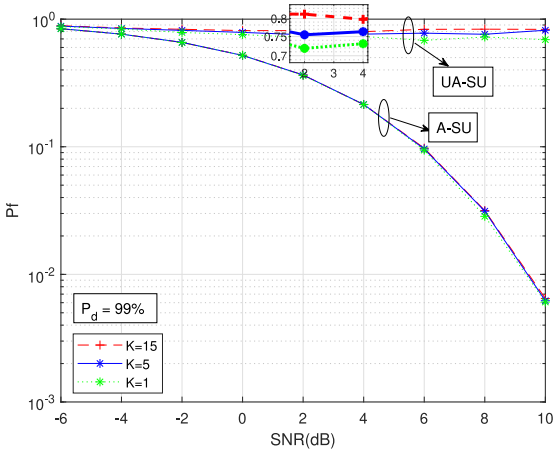

FIGURE 4. Performance of various number of K in SUAC with perfect CSI and $P_{\text{d}} = 99\%$ (Approach I).

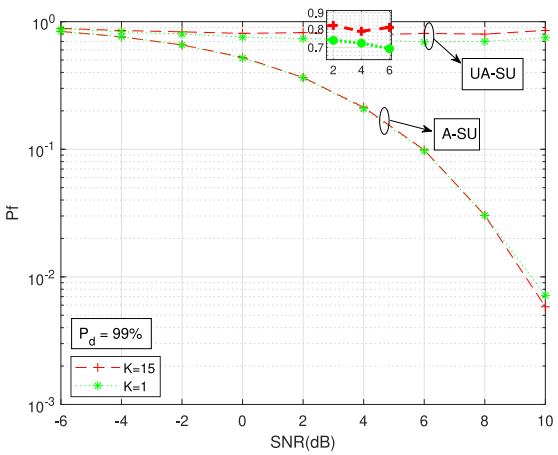

FIGURE 5. Performance of various number of K in SUAC with perfect CSI and $P_{\text{d}} = 99\%$ (Approach II).

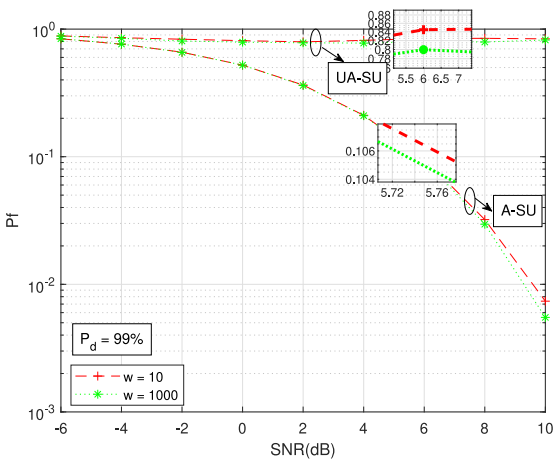

FIGURE 6. Performance of various number of w_i in SUAC with perfect CSI, $P_{\text{d}} = 99\%$, and $K = 5$ (Approach II).

C. DEPENDENT CHANNEL VECTOR BETWEEN A-SUs AND UA-SUs

We consider the spectrum sensing performance when the channel vector of A-SUs ($\mathbf{h}_{\text{a}}$) and UA-SUs ($\mathbf{h}_{\text{ua}}$) are highly dependent for Approach I and II. Specifically, consider there

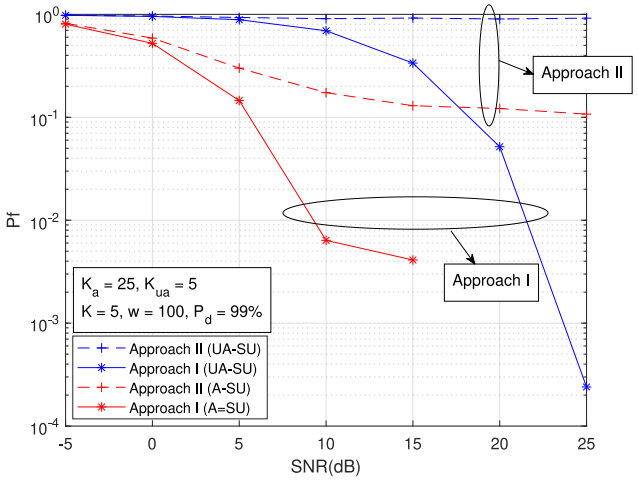

FIGURE 7. Performance of Approach I versus Approach II under dependent channel condition.

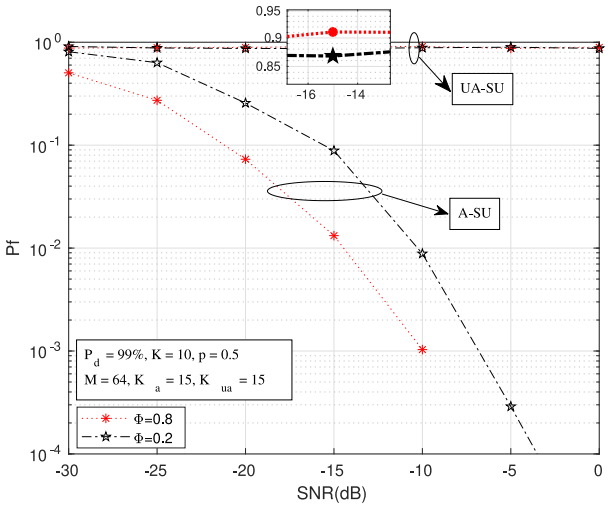

FIGURE 8. Performance of various number of ϕ in SUAC with $p = 0.5$ and $M = 64$ considering iteratively reweighted approach.

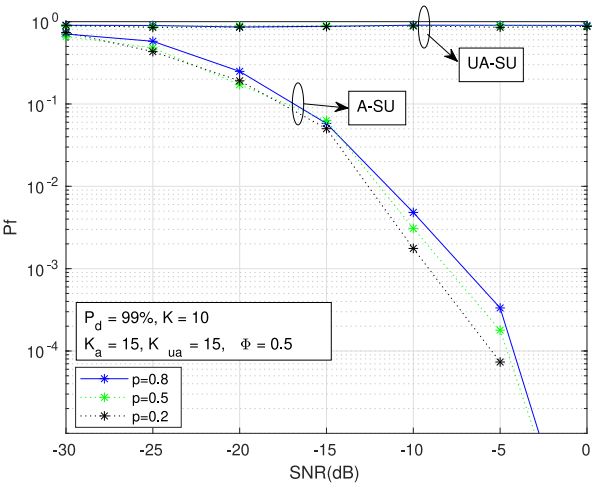

FIGURE 9. Performance of various number of p in SUAC with $\phi = 0.5$ and $M = 64$ considering iteratively reweighted approach.

are 25 A-SUs ($K_a = 25$) and 5 UA-SUs ($K_{ua} = 5$). We first randomly generate the A-SUs channel vector based on the one-ring model and then generate the UA-SUs channel vector by taking a linear combination of the generated A-SUs channel. Fig. 7 presents the A-SU/UA-SU spectrum sensing performance versus SNR given $P_d = 99\%$, $K = 5$, $w_i = 100$, and perfect CSI. From the simulation results, we have the following observations.

1) For Approach I, both A-SUs and UA-SUs spectrum sensing performance improves with increasing SNR value. There will be no secondary user access control given the larger SNR value. Performance is significantly affected due to the channel dependence between A-SU and UA-SU.

2) For Approach II, with increasing SNR value, only A-SUs spectrum sensing performance improved. UA-SU sensing performance is significantly degraded by the proposed algorithm. The channel dependence between A-SUs and UA-SUs will not affect Approach II algorithm effectiveness.

The simulation results verified our design purpose for Approach II. Specifically, if the A-SUs channel vector $\mathbf{h}_a$ and UA-SUs channel vector $\mathbf{h}_{ua}$ are dependent, it will be challenging to generate the jamming signal satisfies the constraints shown in Approach I at the same time. Approach II is designed to address this issue, where the objective function is to minimize the weighted sum of the jamming signal vector squares and the jamming signal influence on K_a A-SUs. Thus, if the channel vectors of A-SUs and UA-SUs are highly correlated or dependent, the spectrum sensing result of Approach II has a much better performance compared to that of Approach I, as shown in Fig. 7.

D. PERFORMANCE OF ITERATIVELY REWEIGHTED ALGORITHMS FOR JAMMING SIGNAL DESIGN

In this section, we show the spectrum sensing performance considering the iterative reweighted algorithms. We consider $L = 30$ SUs (15 A-SUs and 15 UA-SUs), $K = 15$, and $P_d = 99\%$ in our simulation.

Fig. 8 shows the false alarm probability of A-SU/UA-SU versus SNR given $p = 0.5$ (we consider $\ell^{0.5}$-norm) and $M = 64$. The damping parameter ϕ has been investigated with various values, say $\phi = 0.2$ and $\phi = 0.8$. As we discussed in Section VI, the damping parameter ϕ is designed to regularize the optimization process. Without the damping parameter, the weight α_k is undefined whenever $g_k = 0$. Our simulation result shows that a larger value of ϕ ($\phi = 0.8$) corresponds to better jamming performance: A-SU has better spectrum sensing performance while UA-SU has worse sensing performance. Decreasing ϕ too soon results in poorer performance. In our future research, we plan to perform experiments with the ϕ-regularization strategy [19] of using a relatively large ϕ and then repeating the process by decreasing the damping parameter values after convergence to recover the sparse jamming signal.

Fig. 9 and Fig. 10 present the false alarm probability P_f of A-SU/UA-SU versus SNR given $\phi = 0.5$ with various values

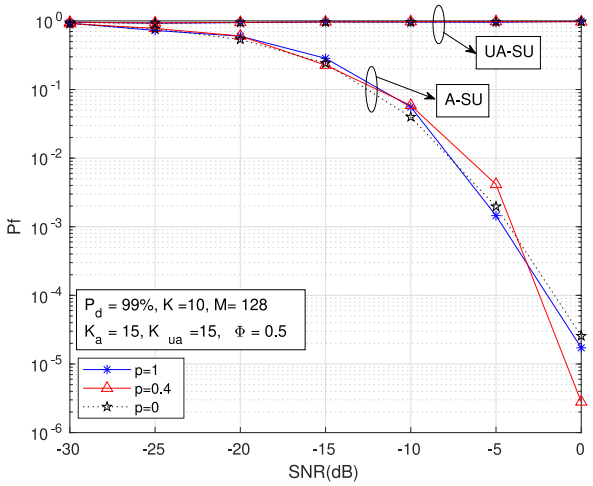

FIGURE 10. Performance of various number of p in SUAC with $\phi = 0.5$ and $M = 128$ considering iteratively reweighted approach.

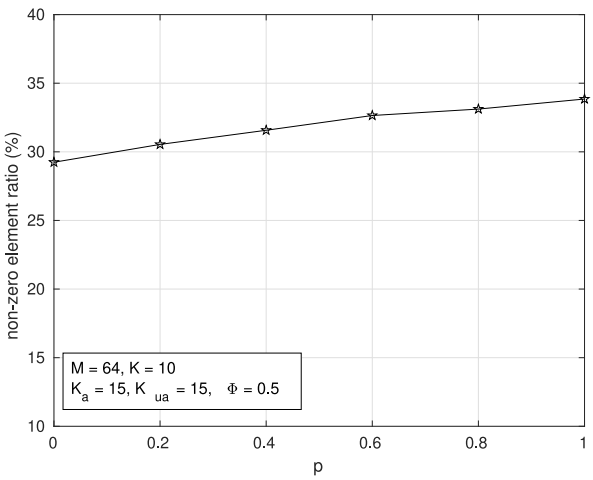

FIGURE 11. Non-zero element ratio versus p value given $\phi = 0.5$ and $M = 64$.

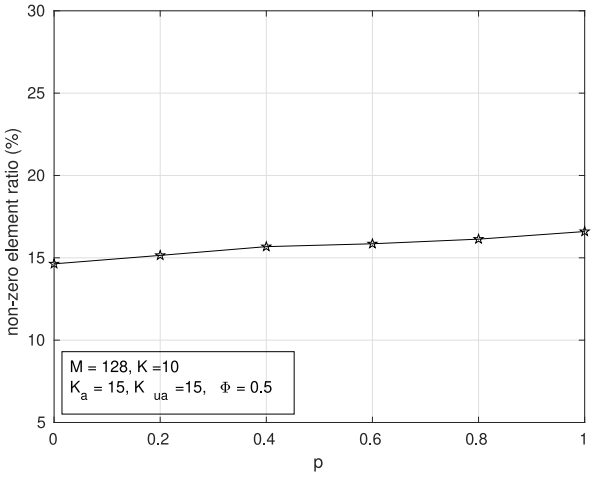

FIGURE 12. Non-zero element ratio versus p value given $\phi = 0.5$ and $M = 128$.

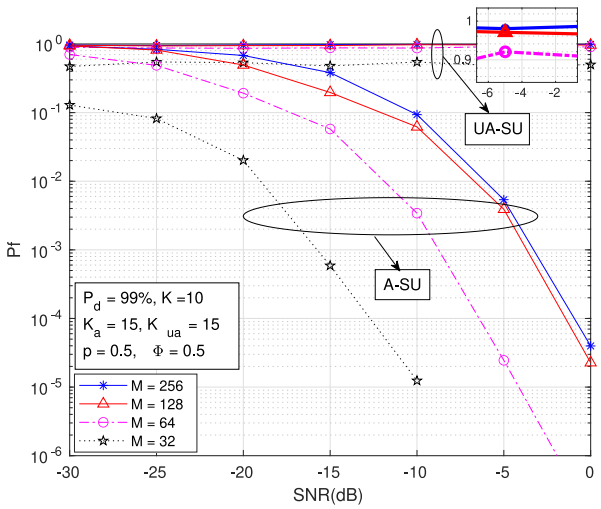

FIGURE 13. Performance of various number of M in SUAC with $p = 0.5$ and $\phi = 0.5$ considering iteratively reweighted approach.

of p. The BS antenna number is $M = 64$ for Fig. 9 and $M = 128$ for Fig. 10. From the simulation results, we can see that there is no significant performance difference among different p values ($p = 0.2, 0.5$, and 0.8). Sparse jamming signal representation (lower p values) will maintain good spectrum sensing performance for A-SUs while introducing a significant impact on UA-SUs with a much lower power cost.

Fig. 11 and Fig. 12 present the non-zero element ratio of the jamming signal versus p value given $\phi = 0.5$. The BS antenna number is $M = 64$ for Fig. 11 and $M = 128$ for Fig. 12. In our simulation, we set the jamming signal element equal to zero whenever the element magnitude is smaller than 10^{-4}, and count the non-zero element number, divide the antenna number M in order to calculate the non-zero element ratio. From Fig. 11 and Fig. 12, we can see that the non-zero element ratio rises with p value increasing for both $M = 64$ and $M = 128$.

In Fig. 13, we present the false alarm probability of A-SU/UA-SU versus SNR given $p = 0.5$ and $\phi = 0.5$ with various BS antenna numbers M. From the simulation results, we have the following observations.

1) For A-SUs, P_f performance improves with the increasing SNR values. Smaller BS antenna number M (i.e., $M = 32$) shows better spectrum sensing performance.

2) For UA-SUs, the spectrum sensing performance is significantly degraded. Larger BS antenna number M (i.e., $M = 256$) shows better jamming performance.

From the above observations, we can see that there is a trade-off between improving spectrum sensing performance on A-SUs and having a powerful jammer on UA-SUs when selecting large or small M values. A larger value of M corresponds to a better jammer while the spectrum sensing performance of A-SUs degrades.

Fig. 14 illustrates the non-zero element ratio of the jamming signal versus BS antenna number M value (i.e., $M = 32, 64, 128, 256$) given $p = 0.5$ and $\phi = 0.5$. From the simulation results, we can see that the non-zero element

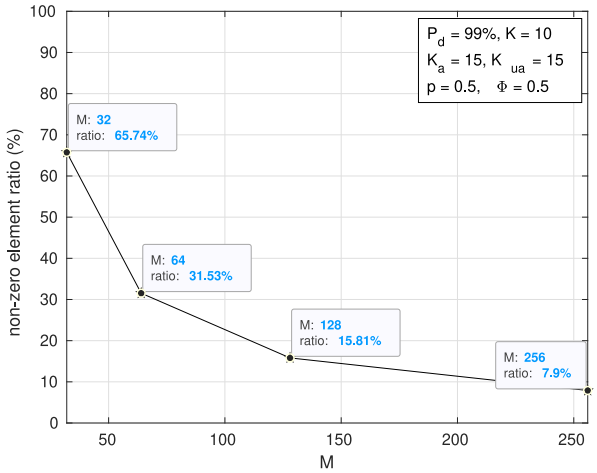

FIGURE 14. Non-zero element ratio versus M value given $p = 0.5$ and $\phi = 0.5$.

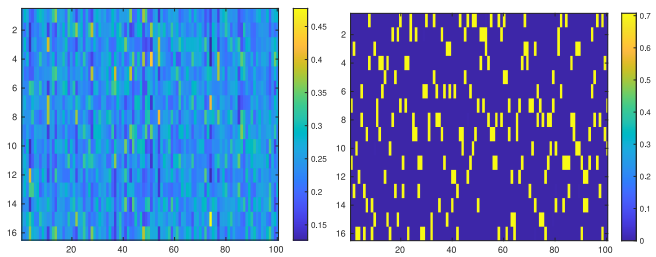

(a) Non-sparse SUAC. (b) Sparse SUAC.

FIGURE 15. Pseudo-color plots for jamming signal weight magnitude.

ratio decreases (the jamming signal becomes sparser) with the M value increasing.

Notice that our proposed iteratively reweighted jamming signal design not only shows equally good or better performance compared with the traditional SUAC method, but we also present a sparse jamming signal weight which leads to a greener system design. The visualization of the jamming signal weights generated from our proposed iteratively reweighted algorithm and traditional SUAC is illustrated in Fig. 15, where we plot the weight magnitude of a 16×100 matrix with $M = 16$ antennas and 100 trails. The figure colors correspond to the data values of the weight matrix and the colorbar on the right indicates the mapping of data values into the colors. From the figure, we can see that our iteratively reweighted approach shows a very sparse jamming signal weight solution.

VIII. CONCLUSION

We proposed a new formulation for jamming signal design that uses the channel state information between SU and PU in a massive MIMO communication architecture. We consider designing the jamming signal process as a non-convex quadratic programming optimization problem and solve this problem via the K-best method. We have shown that A-SUs are able to achieve reliable spectrum sensing performance while UA-SUs suffer significant performance degradation given the carefully designed jamming signal.

APPENDIX A
Eq. (7) DETAILED DERIVATION PROOF

- $\mathbf{h}_{\mathrm{ua},j}^H \mathbf{B}\mathbf{Q}\boldsymbol{\beta} = \sqrt{\tau}\sum_{i=1}^{j} r_{i,S}^* \beta_i$.

Proof: Form (6) we have

$$\mathbf{B}^H[\mathbf{h}_{\mathrm{ua},1},\ldots,\mathbf{h}_{\mathrm{ua},K_{\mathrm{ua}}}]\mathrm{diag}\{1/\sqrt{\tau},\ldots,1/\sqrt{\tau}\} = \mathbf{Q}\mathbf{R} \quad (32)$$

then we have

$$\mathrm{diag}\{1/\sqrt{\tau},\ldots,1/\sqrt{\tau}\}[\mathbf{h}_{\mathrm{ua},1},\ldots,\mathbf{h}_{\mathrm{ua},K_{\mathrm{ua}}}]^H\mathbf{B} = \mathbf{R}^H\mathbf{Q}^H$$
$$\Rightarrow \begin{pmatrix} \frac{1}{\sqrt{\tau}}\mathbf{h}_{\mathrm{ua},1}^H \\ \vdots \\ \frac{1}{\sqrt{\tau}}\mathbf{h}_{\mathrm{ua},K_{\mathrm{ua}}}^H \end{pmatrix}\mathbf{B} = \underbrace{\begin{pmatrix} r_{1,1}^* & 0 & \cdots & 0 \\ r_{1,2}^* & r_{2,2}^* & 0 & \cdots \\ \vdots & \vdots & \ddots & \ddots \\ r_{1,K_{\mathrm{ua}}}^* & r_{2,K_{\mathrm{ua}}}^* & \cdots & r_{K_{\mathrm{ua}},K_{\mathrm{ua}}}^* \end{pmatrix}}_{\mathbf{R}^H}\mathbf{Q}^H \quad (33)$$

from (33) we can see that

$$\mathbf{h}_{\mathrm{ua},j}^H\mathbf{B}\mathbf{Q} = \sqrt{\tau}\left(r_{1,j}^*, r_{2,j}^*, \ldots, r_{j,j}^*, 0, \ldots, 0\right) \quad (34)$$

and we prove that $\mathbf{h}_{\mathrm{ua},j}^H\mathbf{B}\mathbf{Q}\boldsymbol{\beta} = \sqrt{\tau}\sum_{i=1}^{j} r_{i,j}^*\beta_i$.

- $\mathbf{h}_{\mathrm{ua},j}^H\mathbf{B}\tilde{\mathbf{Q}}\tilde{\boldsymbol{\beta}} = 0$.

Proof: Form (33) we have

$$\mathbf{h}_{\mathrm{ua},j}^H\mathbf{B}\tilde{\mathbf{Q}}\tilde{\boldsymbol{\beta}} = \sqrt{\tau}\left(r_{1,j}^*, r_{2,j}^*, \ldots, r_{j,j}^*, 0, \ldots, 0\right)\underbrace{\mathbf{Q}^H\tilde{\mathbf{Q}}}_{\mathbf{0}}\boldsymbol{\beta} = 0 \quad (35)$$

APPENDIX B
PROOF OF PROPOSITION 2

In our following derivations, for expression simplicity, denote $\Theta = \sum_{i=1}^{j-1}|\beta_i|^2 > 0$, $\Phi = |r_{j,j}'| > 0$, and $\Omega = |\sum_{i=1}^{j-1}((r_{i,j}')^*\beta_i)| > 0$. We now have the optimization problem

$$\min_{\tilde{\beta},\tilde{\gamma}\in\mathcal{R}_{\geq 0}} \tilde{\beta}^2 + \Theta\tilde{\gamma}^2 \quad \text{s.t. } \tilde{\gamma} \geq 1,\ \Phi\tilde{\beta} + \Omega\tilde{\gamma} \geq 1 \quad (36)$$

Define the Lagrangian equation as

$$L\left(\tilde{\beta},\tilde{\gamma},\lambda,\mu\right) = \tilde{\beta}^2 + \Theta\tilde{\gamma}^2 + \lambda(1-\tilde{\gamma}) + \mu\left(1-\Phi\tilde{\beta}-\Omega\tilde{\gamma}\right) \quad (37)$$

Then the KKT conditions are

$$\frac{\partial L}{\partial\tilde{\beta}} = 2\tilde{\beta} - \mu\Phi = 0 \quad (38)$$
$$\frac{\partial L}{\partial\tilde{\gamma}} = 2\Theta\tilde{\gamma} - \lambda - \mu\Omega = 0 \quad (39)$$
$$\lambda(1-\tilde{\gamma}) = 0 \quad (40)$$
$$\mu\left(1-\Phi\tilde{\beta}-\Omega\tilde{\gamma}\right) = 0 \quad (41)$$
$$1-\tilde{\gamma} \leq 0 \quad (42)$$
$$1-\Phi\tilde{\beta}-\Omega\tilde{\gamma} \leq 0 \quad (43)$$
$$\lambda \geq 0 \quad (44)$$
$$\mu \geq 0 \quad (45)$$

Case I: $\lambda = 0,\ \mu = 0$.

From (38) and (39) we have $\tilde{\beta} = \tilde{\gamma} = 0$, which contradicts with condition (42) and (43).

Case II: $\lambda = 0,\ \mu > 0$.

From (38) and (39) we have $\tilde{\beta} = \frac{\mu\Phi}{2}$, $\tilde{\gamma} = \frac{\mu\Omega}{2\Theta}$. Since $\mu > 0$, from condition (41) we have

$$\begin{aligned} 1 - \Phi\tilde{\beta} - \Omega\tilde{\gamma} &\equiv 1 - \frac{\mu\Phi^2}{2} - \frac{\mu\Omega^2}{2\Theta} = 0 \\ \Rightarrow \mu &= \frac{2\Theta}{\Theta\Phi^2 + \Omega^2} > 0 \end{aligned} \tag{46}$$

In order to satisfy condition (42), we have

$$\begin{aligned} 1 - \frac{\mu\Omega}{2\Theta} &\equiv 1 - \frac{\Omega}{\Theta\Phi^2 + \Omega^2} \le 0 \\ &\Rightarrow \Theta\Phi^2 + \Omega^2 - \Omega \le 0 \end{aligned} \tag{47}$$

Thus, if Θ, Φ, Ω satisfy $\Theta\Phi^2 + \Omega^2 - \Omega \le 0$, we have $\tilde{\beta}_{\text{opt}} = \frac{\Phi\Theta}{\Theta\Phi^2+\Omega^2}$ and $\tilde{\gamma}_{\text{opt}} = \frac{\Omega}{\Theta\Phi^2+\Omega^2}$.

Case III: $\lambda > 0,\ \mu = 0$.

From (38) and (39) we have $\tilde{\beta} = 0$, $\tilde{\gamma} = \frac{\lambda}{2\Theta}$. Since $\lambda > 0$, from condition (40) we have

$$\begin{aligned} 1 - \tilde{\gamma} &\equiv 1 - \frac{\lambda}{2\Theta} = 0 \\ &\Rightarrow \lambda = 2\Theta > 0 \end{aligned} \tag{48}$$

In order to satisfy (43), we have

$$\begin{aligned} 1 - \Phi\tilde{\beta} - \Omega\tilde{\gamma} &\equiv 1 - \Omega \le 0 \\ &\Rightarrow\ \Omega \ge 1 \end{aligned} \tag{49}$$

Thus, if $\Omega \ge 1$, we have $\tilde{\beta}_{\text{opt}} = 0$ and $\tilde{\gamma}_{\text{opt}} = 1$.

Case IV: $\lambda > 0,\ \mu > 0$.

Since $\lambda > 0$, in order to satisfy condition (40) we have $\tilde{\gamma} = 1$. Similarly, since $\mu > 0$, from (41) we have

$$\begin{aligned} 1 - \Phi\tilde{\beta} - \Omega\tilde{\gamma} &\equiv 1 - \Phi\tilde{\beta} - \Omega = 0 \\ &\Rightarrow\ \tilde{\beta} = \frac{1 - \Omega}{\Phi} \end{aligned} \tag{50}$$

From (38) and (50), we have

$$\begin{aligned} \mu &= \frac{2 - 2\Omega}{\Phi^2} > 0 \\ &\Rightarrow\ \Omega < 1 \end{aligned} \tag{51}$$

and from (39) we can obtain that

$$\begin{aligned} \lambda &= 2\Theta - \mu\Omega \\ &= \frac{2\left(\Theta\Phi^2 + \Omega^2 - \Omega\right)}{\Phi^2} > 0 \\ &\Rightarrow\ \Theta\Phi^2 + \Omega^2 - \Omega > 0 \end{aligned} \tag{52}$$

Thus, if Θ, Φ, Ω satisfy $\Theta\Phi^2 + \Omega^2 - \Omega > 0$ and $\Omega < 1$, we have $\tilde{\beta}_{\text{opt}} = \frac{1-\Omega}{\Phi}$ and $\tilde{\gamma}_{\text{opt}} = 1$.

In conclusion, when Θ, Φ, $\Omega > 0$, we have the following optimal solution

$$\begin{cases} \tilde{\beta}_{\text{opt}} = 0, \tilde{\gamma}_{\text{opt}} = 1 & \text{if } \Omega \ge 1 \\ \tilde{\beta}_{\text{opt}} = \frac{1-\Omega}{\Phi}, \tilde{\gamma}_{\text{opt}} = 1 & \text{if } \Omega < 1, \Theta\Phi^2 + \Omega^2 - \Omega > 0 \\ \tilde{\beta}_{\text{opt}} = \frac{\Phi\Theta}{\Theta\Phi^2+\Omega^2}, \tilde{\gamma}_{\text{opt}} = \frac{\Omega}{\Theta\Phi^2+\Omega^2} & \text{if } \Omega < 1, \Theta\Phi^2 + \Omega^2 - \Omega \le 0 \end{cases} \tag{53}$$

APPENDIX C
PROOF OF PROPOSITION 3

The constraint in (13) can be expanded as

$$\mathbf{h}_{\text{ua},j}^H \mathbf{g} = \mathbf{h}_{\text{ua},j}^H \left(\mathbf{Q}\boldsymbol{\beta} + \tilde{\mathbf{Q}}\tilde{\boldsymbol{\beta}}\right) = \underbrace{\mathbf{h}_{\text{ua},j}^H \mathbf{Q}\boldsymbol{\beta}}_{\text{Part I}} + \underbrace{\mathbf{h}_{\text{ua},j}^H \tilde{\mathbf{Q}}\tilde{\boldsymbol{\beta}}}_{\text{Part II}} \tag{54}$$

We first consider the detailed derivation of Part I in (54). From (14) we have

$$\begin{aligned} &\left[\mathbf{h}_{\text{ua},1}, \ldots, \mathbf{h}_{\text{ua},K_{\text{ua}}}\right] \text{diag}\{1/\sqrt{\tau}, \ldots, 1/\sqrt{\tau}\}, \left[\mathbf{h}_{\text{a},1}, \ldots, \mathbf{h}_{\text{a},K_{\text{a}}}\right] \\ &= \mathbf{QR} \end{aligned} \tag{55}$$

then we have

$$\begin{pmatrix} \frac{1}{\sqrt{\tau}}\mathbf{h}_{\text{ua},1}^H \\ \vdots \\ \frac{1}{\sqrt{\tau}}\mathbf{h}_{\text{ua},K_{\text{ua}}}^H \\ \mathbf{h}_{\text{a},1}^H \\ \vdots \\ \mathbf{h}_{\text{a},K_{\text{a}}}^H \end{pmatrix} = \underbrace{\begin{pmatrix} r_{1,1}^* & 0 & \cdots & \cdots & \cdots & 0 \\ \vdots & \ddots & \ddots & \ddots & \ddots & \vdots \\ r_{1,K_{\text{ua}}}^* & \cdots & r_{K_{\text{ua}},K_{\text{ua}}}^* & 0 & \cdots & \vdots \\ r_{1,K_{\text{ua}}+1}^* & \cdots & \cdots & r_{K_{\text{ua}}+1,K_{\text{ua}}+1}^* & 0 & \vdots \\ \vdots & \ddots & \ddots & \ddots & \ddots & \vdots \\ r_{1,L}^* & \cdots & \cdots & \cdots & \cdots & r_{L,L}^* \end{pmatrix}}_{\mathbf{R}^H} \mathbf{Q}^H \tag{56}$$

from (56) we have

$$\begin{aligned} \mathbf{h}_{\text{ua},j}^H \mathbf{Q} &= \sqrt{\tau}\left(r_{1,j}^*, r_{2,j}^*, \ldots, r_{j,j}^*, 0, \ldots, 0\right) \underbrace{\mathbf{Q}^H\mathbf{Q}}_{\mathbf{I}} \\ \mathbf{h}_{\text{a},i}^H \mathbf{Q} &= \left(r_{1,K_{\text{ua}}+i}^*, r_{2,K_{\text{ua}}+i}^*, \ldots, r_{K_{\text{ua}}+i,K_{\text{ua}}+i}^*, 0, \ldots, 0\right) \underbrace{\mathbf{Q}^H\mathbf{Q}}_{\mathbf{I}} \end{aligned} \tag{57}$$

from (57) we have

$$\mathbf{h}_{\text{ua},j}^H \mathbf{Q}\boldsymbol{\beta} = \sqrt{\tau} \sum_{k=1}^{j} r_{k,j}^* \beta_k,\ \mathbf{h}_{\text{a},i}^H \mathbf{Q}\boldsymbol{\beta} = \sum_{k=1}^{K_{\text{ua}}+i} r_{k,K_{\text{ua}}+i}^* \beta_k \tag{58}$$

Part II in (54) $\mathbf{h}_{\text{ua},j}^H \tilde{\mathbf{Q}}\tilde{\boldsymbol{\beta}} = 0$ which can be easily obtained as

$$\mathbf{h}_{\text{ua},j}^H \tilde{\mathbf{Q}}\tilde{\boldsymbol{\beta}} = \sqrt{\tau}\left(r_{1,j}^*, r_{2,j}^*, \ldots, r_{j,j}^*, 0, \ldots, 0\right) \underbrace{\mathbf{Q}^H\tilde{\mathbf{Q}}}_{\mathbf{0}} \tilde{\boldsymbol{\beta}} = 0 \tag{59}$$

Also, we have

$$\begin{aligned} \mathbf{h}_{\text{a},i}^H \tilde{\mathbf{Q}}\tilde{\boldsymbol{\beta}} &= \left(r_{1,K_{\text{ua}}+i}^*, r_{2,K_{\text{ua}}+i}^*, \ldots, r_{K_{\text{ua}}+i,K_{\text{ua}}+i}^*, 0, \ldots, 0\right) \underbrace{\mathbf{Q}^H\tilde{\mathbf{Q}}}_{\mathbf{0}} \tilde{\boldsymbol{\beta}} \\ &= 0 \end{aligned} \tag{60}$$

From (58) and (59) we have $\mathbf{h}_{\text{ua},j}^H \mathbf{g} = \sqrt{\tau} \sum_{k=1}^{j} r_{k,j}^* \beta_k$, none of the constraints depend on $\tilde{\boldsymbol{\beta}}$ and we complete our proof.

APPENDIX D
PROCEDURES TO SOLVE (31)

In this section, we provide detailed procedures to solve the non-convex optimization problem (31). For explanation convenience, we ignore the time step indicator t in the original problem expression and rewrite the problem as follows

$$\begin{aligned} \min_{\mathbf{g}\in\mathcal{C}^{M\times 1}} \quad & w_0\|\Upsilon^{\frac{1}{2}}\mathbf{g}\|^2 + \sum_{i=1}^{K_{\mathrm{a}}} w_i\|\mathbf{h}_{\mathrm{a},i}^H\mathbf{g}\|^2 \\ \text{s.t.} \quad & \|\mathbf{h}_{\mathrm{ua},j}^H\mathbf{g}\|^2 \geq \tau,\ j=1,\ldots,K_{\mathrm{ua}} \end{aligned} \tag{61}$$

Denote $\tilde{\mathbf{g}} \triangleq \Upsilon^{\frac{1}{2}}\mathbf{g}$ with dimension $M\times 1$, and we then have $\mathbf{g} = \Upsilon^{-\frac{1}{2}}\tilde{\mathbf{g}}$. The optimization problem (61) can be rewritten as

$$\begin{aligned} \min_{\tilde{\mathbf{g}}\in\mathcal{C}^{M\times 1}} \quad & w_0\|\tilde{\mathbf{g}}\|^2 + \sum_{i=1}^{K_{\mathrm{a}}} w_i\|\mathbf{h}_{\mathrm{a},i}^H\Upsilon^{-\frac{1}{2}}\tilde{\mathbf{g}}\|^2 \\ \text{s.t.} \quad & \|\mathbf{h}_{\mathrm{ua},j}^H\Upsilon^{-\frac{1}{2}}\tilde{\mathbf{g}}\|^2 \geq \tau,\ j=1,\ldots,K_{\mathrm{ua}} \end{aligned} \tag{62}$$

We then denote $\tilde{\mathbf{h}}_{\mathrm{a},i}^H \triangleq \mathbf{h}_{\mathrm{a},i}^H\Upsilon^{-\frac{1}{2}}$ and $\tilde{\mathbf{h}}_{\mathrm{ua},j}^H \triangleq \mathbf{h}_{\mathrm{ua},j}^H\Upsilon^{-\frac{1}{2}}$, and optimization problem (62) can be expressed as

$$\begin{aligned} \min_{\tilde{\mathbf{g}}\in\mathcal{C}^{M\times 1}} \quad & w_0\|\tilde{\mathbf{g}}\|^2 + \sum_{i=1}^{K_{\mathrm{a}}} w_i\|\tilde{\mathbf{h}}_{\mathrm{a},i}^H\tilde{\mathbf{g}}\|^2 \\ \text{s.t.} \quad & \|\tilde{\mathbf{h}}_{\mathrm{ua},j}^H\tilde{\mathbf{g}}\|^2 \geq \tau,\ j=1,\ldots,K_{\mathrm{ua}} \end{aligned} \tag{63}$$

which is the same as the problem shown in (13). We then follow the proposed K-best algorithm to solve problem (63) and obtain $\tilde{\mathbf{g}}_{\mathrm{opt}}$. The corresponded optimal value of $\mathbf{g}$ at this iteration is given as $\mathbf{g}_{\mathrm{opt}} = \Upsilon^{-\frac{1}{2}}\tilde{\mathbf{g}}_{\mathrm{opt}}$.

REFERENCES

[1] J. Mitola and G. Q. Maguire, "Cognitive radio: Making software radios more personal," *IEEE Pers. Commun.*, vol. 6, no. 4, pp. 13–18, Aug. 1999.

[2] R. Tandra, S. M. Mishra, and A. Sahai, "What is a spectrum hole and what does it take to recognize one?" *Proc. IEEE*, vol. 97, no. 5, pp. 824–848, May 2009.

[3] T. Yucek and H. Arslan, "A survey of spectrum sensing algorithms for cognitive radio applications," *IEEE Commun. Surveys Tuts.*, vol. 11, no. 1, pp. 116–130, 1st Quart., 2009.

[4] R. Chen, J.-M. Park, and J. H. Reed, "Defense against primary user emulation attacks in cognitive radio networks," *IEEE J. Sel. Areas Commun.*, vol. 26, no. 1, pp. 25–37, Jan. 2008.

[5] R. Chen, J.-M. Park, Y. T. Hou, and J. H. Reed, "Toward secure distributed spectrum sensing in cognitive radio networks," *IEEE Commun. Mag.*, vol. 46, no. 4, pp. 50–55, Apr. 2008.

[6] N. Hu, Y.-D. Yao, and J. Mitola, "Most active band (MAB) attack and countermeasures in a cognitive radio network," *IEEE Trans. Wireless Commun.*, vol. 11, no. 3, pp. 898–902, Mar. 2012.

[7] H. Wang, Y.-D. Yao, X. Zhang, and H. Li, "Secondary user access control in cognitive radio networks," *IEEE J. Sel. Areas Commun.*, vol. 34, no. 11, pp. 2866–2873, Nov. 2016.

[8] H. Wang, Y.-D. Yao, and S. Peng, "Prioritized secondary user access control in cognitive radio networks," *IEEE Access*, vol. 6, pp. 11007–11016, 2018.

[9] H. Wang, Y.-D. Yao, H. Li, and H. Xia, "Secondary user access control with MassiveMIMO in cognitive radio networks," in *Proc. IEEE Int. Symp. Dyn. Spectr. Access Netw. (DySPAN)*, 2019, pp. 1–9.

[10] Z.-Q. Luo, W.-K. Ma, A. M.-C. So, Y. Ye, and S. Zhang, "Semidefinite relaxation of quadratic optimization problems," *IEEE Signal Process. Mag.*, vol. 27, no. 3, pp. 20–34, May 2010.

[11] S. Boyd, S. P. Boyd, and L. Vandenberghe, *Convex Optimization*. Cambridge, U.K.: Cambridge Univ. Press, 2004.

[12] M. Zibulevsky and M. Elad, "L1–L2 optimization in signal and image processing," *IEEE Signal Process. Mag.*, vol. 27, no. 3, pp. 76–88, May 2010.

[13] E. J. Candès, J. Romberg, and T. Tao, "Robust uncertainty principles: Exact signal reconstruction from highly incomplete frequency information," *IEEE Trans. Inf. Theory*, vol. 52, no. 2, pp. 489–509, Feb. 2006.

[14] Z. Qin, J. Fan, Y. Liu, Y. Gao, and G. Y. Li, "Sparse representation for wireless communications: A compressive sensing approach," *IEEE Signal Process. Mag.*, vol. 35, no. 3, pp. 40–58, May 2018.

[15] Y. Han, J. Lee, and D. J. Love, "Compressed sensing-aided downlink channel training for FDD massive MIMO systems," *IEEE Trans. Commun.*, vol. 65, no. 7, pp. 2852–2862, Jul. 2017.

[16] Y. C. Eldar, P. Kuppinger, and H. Bolcskei, "Block-sparse signals: Uncertainty relations and efficient recovery," *IEEE Trans. Signal Process.*, vol. 58, no. 6, pp. 3042–3054, Jun. 2010.

[17] L. Kong, D. Zhang, Z. He, Q. Xiang, J. Wan, and M. Tao, "Embracing big data with compressive sensing: A green approach in industrial wireless networks," *IEEE Commun. Mag.*, vol. 54, no. 10, pp. 53–59, Oct. 2016.

[18] N. Prasad, Q. Zhang, and X. F. Qi, "Channel reconstruction via quadratic programming in massive MIMO networks," in *Proc. Int. Symp. Model. Optim. Mobile Ad Hoc Wireless Netw. (WiOPT)*, 2019, pp. 1–8.

[19] R. Chartrand, "Exact reconstruction of sparse signals via nonconvex minimization," *IEEE Signal Process. Lett.*, vol. 14, no. 10, pp. 707–710, Oct. 2007.

[20] R. Chartrand and W. Yin, "Iteratively reweighted algorithms for compressive sensing," in *Proc. IEEE Int. Conf. Acoust. Speech Signal Process.*, 2008, pp. 3869–3872.

[21] E. J. Candes, M. B. Wakin, and S. P. Boyd, "Enhancing sparsity by reweighted ℓ^1 minimization," *J. Fourier Anal. Appl.*, vol. 14, no. 5, pp. 877–905, 2008.

[22] C. Shepard et al., "Argos: Practical many-antenna base stations," in *Proc. 18th Annu. Int. Conf. Mobile Comput. Netw.*, 2012, pp. 53–64.

[23] Z. Gao, L. Dai, Z. Wang, and S. Chen, "Spatially common sparsity based adaptive channel estimation and feedback for FDD massive MIMO," *IEEE Trans. Signal Process.*, vol. 63, no. 23, pp. 6169–6183, Dec. 2015.

[24] J. Fang, X. Li, H. Li, and F. Gao, "Low-rank covariance-assisted downlink training and channel estimation for FDD massive MIMO systems," *IEEE Trans. Wireless Commun.*, vol. 16, no. 3, pp. 1935–1947, Mar. 2017.

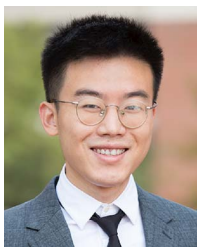

HUAXIA WANG (Member, IEEE) received the B.Eng. degree in information engineering from Southeast University, Nanjing, China, in 2012, and the Ph.D. degree in electrical engineering from the Stevens Institute of Technology, Hoboken, NJ, USA, in 2018. In 2016 and 2017, he was a Research Intern with the Mathematics of Networks and Systems Research Department, Nokia Bell Labs, Murray Hill, NJ, USA. He joined Futurewei Technologies, Inc., Bridgewater, NJ, USA, in 2018. He is currently working as an Assistant Professor with Oklahoma State University, Stillwater, OK, USA. His research interests include image processing, wireless communications, cognitive radio networks, reinforcement learning, and deep learning. He was the recipient of the Outstanding Ph.D. Dissertation Award in electrical engineering and the Edward Peskin Award with the Stevens Institute of Technology in 2018.

YU-DONG YAO (Fellow, IEEE) received the B.Eng. and M.Eng. degrees in electrical engineering from the Nanjing University of Posts and Telecommunications, Nanjing, China, in 1982 and 1985, respectively, and the Ph.D. degree in electrical engineering from Southeast University, Nanjing, in 1988. Since 2000, he has been with the Stevens Institute of Technology, Hoboken, NJ, USA, where he is currently a Professor with the Department of Electrical and Computer Engineering. His research interests include wireless communications, machine learning and deep learning techniques, and healthcare and medical applications. He has served as an Associate Editor for the IEEE COMMUNICATIONS LETTERS from 2000 to 2008 and the IEEE TRANSACTIONS ON VEHICULAR TECHNOLOGY from 2001 to 2006. He has served as an Editor for the IEEE TRANSACTIONS ON WIRELESS COMMUNICATIONS from 2001 to 2005. For his contributions to wireless communications systems, he was elected as a Fellow of the National Academy of Inventors in 2015 and the Canadian Academy of Engineering in 2017.